Nature Reviews Earth & Environment
September 2023, Volume 4, Pages 642-658
https://doi.org/10.1038/s43017-023-00458-1
https://archimer.ifremer.fr/doc/00849/96122/

Detailed monitoring reveals the nature of submarine turbidity currents

Talling Peter J. [1,*], Cartigny Matthieu J. B. [2], Pope Ed [2], Baker Megan [2], Clare Michael A. [3], Heijnen Maarten [4], Hage Sophie [12], Parsons Dan R. [6], Simmons Steve M. [6], Paull Charlie K. [7], Gwiazda Roberto [7], Lintern Gwyn [8], Hughes Clarke John E. [9], Xu Jingping [10], Silva Jacinto Ricardo [5], Maier Katherine L. [11]

[1] Departments of Geography and Earth Sciences, University of Durham, Durham, UK
[2] Department of Geography, University of Durham, Durham, UK
[3] Ocean BioGeosciences Group, National Oceanography Centre, Southampton, UK
[4] School of Ocean and Earth Sciences, University of Southampton, Southampton, UK
[5] Geo-Ocean, University of Brest, CNRS, IFREMER, Plouzané, France
[6] Energy and Environment Institute, University of Hull, Hull, UK
[7] Monterey Bay Aquarium Research Institute, Moss Landing, CA, USA
[8] Geological Survey of Canada, Natural Resources Canada, Sidney, British Columbia, Canada
[9] University of New Hampshire, Durham, NH, USA
[10] Southern University of Science and Technology, Guangdong, China
[11] National Institute of Water and Atmospheric Research Te Whanganui-a-Tara Wellington, Aotearoa, New Zealand
[12] Geo-Ocean, University of Brest, CNRS, IFREMER, Plouzané, France

* Corresponding author : Peter J. Talling, email address : Peter.J.Talling@durham.ac.uk

Abstract :

Seafloor sediment flows, called turbidity currents, form the largest sediment accumulations, deepest canyons and longest channels on Earth. It was once thought that turbidity currents were impractical to measure in action, especially given their ability to damage sensors in their path, but direct monitoring since the mid-2010s has measured them in detail. In this Review, we summarize knowledge of turbidity currents gleaned from this direct monitoring. Monitoring identifies triggering mechanisms from dilute river plumes, and shows how rapid sediment accumulation can precondition slope failure, but the final triggers can be delayed and subtle. Turbidity currents are consistently more frequent than predicted by past sequence-stratigraphic models, including at sites >300 km from any coast. Faster flows (more than ~1.5 m s–1) are driven by a dense near-bed layer at their front, whereas slower flows are entirely dilute. This frontal layer sometimes erodes large (>2.5 km3) volumes of sediment, yet maintains a near-uniform speed, leading to a travelling-wave model. Monitoring shows that flows sculpt canyons and channels through fast-moving knickpoints, and shows how deposits originate. Emerging technologies with reduced cost and risk can lead to widespread monitoring of turbidity currents, so their sediment and carbon fluxes can be compared with other major global transport processes.

Keywords : Natural hazards, Ocean sciences, Sedimentology

Introduction

Turbidity currents are mixtures of sediment and water that travel downslope because they are denser than the surrounding water [1]. They are fascinating due to their prodigious scale and power (Fig. 1; Supplementary Table 1). For example, a turbidity current that broke all telecommunication cables across the NW Atlantic in 1929 had a sediment volume of about 200 km^3 [2,3], which is ~30 times the global annual sediment flux from all rivers, and bigger than the largest subaerial landslide in the last 350,000 years (Fig 1b; Supplementary Table 1). These cable breaks showed the 1929 flow travelled at speeds of up to 19 m/s and ran out for over 800 km (Fig. 1a) [2,3]. In 2020, turbidity currents initiated at the mouth of the Congo River travelled for > 1,100 km through the Congo Submarine Canyon offshore West Africa [4] (Fig. 1a). These flows accelerated from 5 to 8 m/s and eroded ~2.65 km^3 of sediment (Fig. 1b). They broke both seabed telecommunication cables to West Africa, causing the internet to slow from Nigeria to South Africa, just when capacity was most needed during Covid-19 related lockdowns [4,5].

Turbidity currents have wider importance for many reasons. As shown by the 1929 NW Atlantic and 2020 Congo Canyon flows, turbidity currents commonly break networks of seabed telecommunication cables [2-7] that now carry over 99% of global intercontinental data traffic, as they have much greater bandwidth than satellites [7]. These cables form the backbone of the internet, and they are critical for many aspects of our daily lives, from intercontinental phone traffic to financial markets and cloud data storage [7]. Turbidity currents also play an important role in transfer and burial of fresh organic carbon in marine sediments, which remove CO_2 from the atmosphere, regulating climate over geologic time scales [8-10] (Fig. 2b,c). It was once thought that terrestrial organic carbon supplied to the oceans was mainly oxidized on continental shelves [11-13], and turbidity currents were omitted from analyses of global carbon cycles [11-13]. However, recent work suggests burial of terrestrial organic via turbidity currents can be highly efficient [8,9], and global estimates of organic carbon burial in marine sediments may thus need to be revisited (Fig. 2b) [14].

Organic carbon is also the basis for all non-chemosynthetic marine food webs, and turbidity currents may thus play a key role in functioning of seabed ecosystems [15,16]. Rapid and sustained deposition of organic-carbon-rich sediment by turbidity currents can also favour chemosynthetic communities [16], whilst sometimes extremely powerful flows may scour life from the seafloor [5,17]. Turbidity currents and their carbon transport are linked to human activities, as they can be generated by seabed trawling [18], or transfer microplastics and other pollutants into the deep-sea [19]. Turbidity current deposits (called turbidites) also provide a record of Earth history. This potentially includes long-term and therefore valuable records of other important geohazards such as major earthquakes [20-22], or river-floods [4]; although it can be very challenging to infer the triggering mechanism for an ancient turbidite with confidence. Thick and extensive turbidite deposits in the rock record also host major oil and gas reserves in many locations worldwide [23].

Major advances in understanding have previously been made using analyses of rock outcrops, seabed cores, and turbidity currents within laboratory experiments or numerical models [e.g. 1,24-26]. But the most remarkable aspect of submarine turbidity currents is how few direct measurements we previously had from these flows [27-31], ensuring that they were poorly understood [32]. Indeed, it was once thought to be impractical [33] to measure turbidity currents directly in the oceans, due to their location, infrequent occurrence, and ability to badly damage (or entirely remove) sensors left in their path.

However, over the last decade or so, a series of ambitious projects have used new sensors and methods to provide the first detailed measurements within submarine turbidity currents (Fig. 4). They have consistently used acoustic Doppler current profilers (ADCPs) mounted on moorings (Fig. 4e) to measure flow velocity profiles at frequencies of seconds to minutes, including at multiple places along the flow pathway [34-53]. Projects were initially conducted in shallow (< 500m) water [38,39], where logistics are easier and costs lower, before moving into deeper (up to 2 km) water [35-37], and then finally capturing extremely large events that reach water depths of 4-5 km [4] (Fig. 4b-d). Direct flow monitoring has been combined with detailed time-lapse mapping of the seabed [35,38,39,54], tracking of heavy objects (Fig. 4f) [35,52], sediment traps inside the flow [41-42,51], and coring of seabed deposits [50,51] to make significant advances in our understanding of how turbidity currents work. These projects have not been without challenges and risks, such as needing to recover broken moorings drifting across the ocean surface near the Congo Canyon before their locator beacons stopped transmitting, all during a Covid-19 related lockdown [4,5], finding and recovering severed and buried cabled infrastructure [48], or when turbidity currents occurred only on the last days of field campaigns [50].

This paper is the story of what recent direct monitoring studies can tell us about these fascinating flows. It addresses some of the most fundamental questions about turbidity currents, which include: (1) How are turbidity currents caused, and how reliably do they record other major geohazards (e.g. earthquakes or floods)? (2) How frequent are turbidity currents, and what are the wider implications for organic carbon cycles (Fig. 2)? (3) What are turbidity currents: entirely dilute suspensions or driven by dense near-bed layers? (4) How do flows evolve and behave? (5) How do flows sculpt the seafloor, and (6) how are turbidity currents recorded by their deposits? It finishes with brief suggestions for key future work.

Causes of turbidity currents

Turbidity currents are caused by four general types of processes [55,56] (Fig. 5a). First, turbidity currents can form from disintegration of underwater landslides [3,55,56] that may have a variety of preconditioning factors (e.g. rapid sediment accumulation) and final triggers (e.g. earthquakes or repeated wave loading). Second, turbidity currents may originate via sediment-laden river discharge that is denser than seawater, and thus plunges to move along the seabed as a 'hyperpycnal flow' [58] (Fig. 5a), although such conditions are rare. Third, sediment settling from surface river plumes with much lower sediment concentrations than hyperpycnal flows may generate turbidity currents [39,58] (Fig. 5a). Fourth, turbidity currents can be initiated by oceanographic processes that transfer sediment to canyon heads, which may be located far from river mouths [27,55,56]. Oceanographic processes include storm waves and tides, or internal waves that move along density interfaces within the ocean (Fig. 5a) [27,55,56].

Recent direct monitoring shows that generation of turbidity currents by surface river plumes can occur at a far wider range of river mouths than once thought. It was previously believed that it only occurred when sediment concentrations in rivers exceeded 1 kg/m^3. However, monitoring at Squamish Delta (Canada) showed that surface river plumes with sediment concentrations as low as 0.07 kg/m^3 can generate frequent turbidity currents [39], sometimes even more frequently than landslide-triggered turbidity currents [59]. This means that a much larger fraction of river mouths globally have the potential to cause turbidity currents [39]. The exact mechanism by which turbidity currents originate below such dilute surface plumes is still uncertain, but it may be linked to generation of mobile fluid-mud-like layers on the seabed [39,47,48], or sediment trapping via estuarine circulation, or both [39].

Direct monitoring also shows that turbidity currents are caused in many locations by a combination of river floods and tidal cycles (Fig. 5b-d), representing both riverine and oceanographic processes. At both Squamish Delta and nearby Fraser Delta in British Columbia, Canada, turbidity current activity switches on above a threshold river discharge, and turbidity currents tend to occur at spring low-tides that produce stronger offshore directed river plumes, in combination with easily remobilised seafloor mud layers [38,39,47,48]. Timing of exceptionally large turbidity currents in Congo Canyon offshore West Africa show they are associated with major (1-in-50-year) river floods (Fig. 5c). However, these turbidity currents finally occurred several weeks to months after the Congo River's flood peak (Fig. 5c), typically at spring tides [4] (Fig. 5d).

Thus, there may be significant time delays after river floods before the turbidity currents are eventually triggered (Fig. 5b). Submarine canyon heads can act as sediment 'capacitors', which are later discharged, often due to a rather minor external perturbation such as spring tides (fig. 5d) [4,60]. For example, multiple huge canyon-flushing flows in Congo Canyon occurred several weeks or months after a river flood peak (Fig. 5c) [4], and a similar pattern is seen elsewhere, albeit with shorter delays. For example, a turbidity current occurred 2-3 days after a huge flood along the Gaoping River in Taiwan [6], whilst landslide-triggered turbidity currents occurred hours after the flood peak at the Squamish Delta [61]. It appears that sediment builds up and stays on the seabed, before a final, often subtle trigger [4,60,61] (Fig. 5b). Such delays therefore complicate the relationship between the timing of major external events (e.g. floods and earthquakes) and turbidity currents. Indeed, in a few cases, direct measurements shows that turbidity currents may be triggered without any obvious synchronous external trigger. A turbidity current that moved at 4-7 m/s and ran out for 50 km in Monterey Canyon occurred on a day without a storm, river flood or earthquake [60].

Triggers of 'canyon-flushing' events are especially important because it has been proposed that deep-sea turbidites can record major earthquakes in some settings. If reliable, turbidite paleo-seismology would be valuable, as these marine records can go back further in time than almost all records on land [20-22]. However, care is needed as there are potential pitfalls. Earthquake triggered turbidites need to be distinguished reliably from turbidites triggered in many other ways, and we need to test whether all or only some major earthquakes trigger distinctive turbidity currents [21,22]. It has been proposed that only earthquakes produce synchronous turbidites over very extensive (>100 km) areas [20]. However, correlating individual turbidite layers over such distances is challenging, especially for ancient layers if uncertainties in radiocarbon dates are similar to earthquake recurrence intervals [20,22], and tropical cyclones also affect very large areas [22]. Turbidites with multiple fining-upward pulses have been linked to peaks in ground motion during earthquakes [20], but turbidity currents with multiple pulses can also be generated by river floods [36,37,46]. Repeated earthquake shaking may also potentially cause sediment to consolidate and become stronger in some locations [62]. However, significant advances have been made in 'testing the tests' for earthquake triggered turbidites, and understanding which sites are better suited for turbidite paleoseismology. For example, Howarth et al. [21] showed there was a consistent spatial relationship between earthquake ground motions during the 2016 Kaikōura earthquake and coseismic turbidites. McHugh et al. [63] also showed how the M_w 9 Tohoku-Oki earthquake offshore Japan in 2011 remobilised a layer of surface sediment that was just a few centimeters thick. Exceptionally well-dated turbidites in varved lakes can be correlated with confidence and provide compelling evidence for earthquake triggering [64].

Direct monitoring also tests how turbidity currents may record major river floods [46,58]. At least offshore from the Congo River, a single river flood may produce a cluster of multiple turbidity currents in following years [4] (Fig. 5c). Direct monitoring of the Var system in the Mediterranean showed how (non-earthquake) landslides and floods may produce turbidity currents with multiple pulses, such that multi-pulsed deposits are not a unique criterion for identifying earthquake or flood triggering [46]. Finally, turbidites may provide important insights into how volcanic islands collapse [65], and whether this occurs in one or multiple stages, which is critically important for tsunami magnitude.

Flow frequency and its wider implications

Direct monitoring of turbidity currents has consistently found that turbidity currents are more frequent than previously expected (Fig. 3e; Supplementary Fig. 1), such as by sequence stratigraphic models [66] (Fig. 3c,d). These sequence stratigraphic models infer that most modern turbidity current systems are inactive, and that activity is mainly restricted to periods of falling or low global sea-level (Fig. 3c) [66]. This is because post-glacial sea-level rise has flooded continental shelves, causing almost all submarine canyon-heads to become detached from river mouths (Fig. 3d), so that only ~180 of ~9,500 submarine canyons currently extend to within 6 km of shore [67,68].

However, direct monitoring now shows that modern-day turbidity current systems in a range of settings can be highly active. For example, over 100 turbidity currents occurred on Squamish Pro-delta in Canada in ~3 months [38,39,59,61], whilst turbidity currents in the upper Congo Canyon lasted for over a week (Supplementary Fig. 1d) and are active ~30% of the time [36,37]. Turbidity currents occurred even in canyons fed by rocky shorelines that lack obvious sediment sources [43]. More powerful canyon-flushing turbidity currents may also be more frequent than once thought, as they can be linked to river floods with recurrence intervals of a few decades (Fig. 5c) [4], as well as major earthquakes with longer recurrence intervals [17]. Frequent and powerful flows were also measured outside of submarine canyons and channels. For example, dozens of flows occurred on the open-slope of the Fraser Pro-delta, some with velocities of > 6 m/s [47,48]. Most surprisingly, it was found that 4-6 powerful (5-8 m/s) flows occurred in Whittard Canyon each year, despite this canyon being >300 km from the nearest shoreline [69] (Supplementary Fig. 1a-c). Indeed, Whittard Canyon in the N.E. Atlantic is as active as Monterey Canyon in California, whose head is located tens of meters from the shoreline [15,35]. There are several thousand other 'shoreline-detached' canyons similar to Whittard Canyon [67,68], and this raises the question of their flow activity [69].

Direct monitoring is thus consistent with some previous studies that challenged prevailing models of dormant turbidity current systems during sea-level [e.g. 70] (Fig. 3d). Other lines of evidence than direct monitoring also suggest that turbidity currents may transfer sediment efficiently to the deep-sea, even when submarine canyon heads are not located within a few kilometers of river mouths (Fig. 3e). Prograding wedges of sediment (clinoforms) offshore from major rivers can reach canyon heads (Fig. 3e). This is the case for the huge Ganges-Brahmaputra River that alone supplies ~16% of all riverine sediment to the ocean [71] (Fig. 2d), with dated cores showing a submarine canyon-head some 130 km from the river mouth is highly active [72]. Oceanographic processes likely play a key role in producing these highly active turbidity current systems located far from river mouths. For example, waves and tides may resuspend sediment and transport it efficiently across continental shelves to submarine canyons [73], as documented by studies of the continental shelf offshore from the Eel River that show 70-80% of sediment was lost over the shelf edge (Fig. 3e) [74].

Thus, the present-day turbidity current ‘pump’ may be much more active than once thought (Figs. 2 & 3e). This may have significant wider implications for transfer and burial of organic carbon in the deep-sea [8,14], which affects atmospheric CO_2 levels and thus climate over long (> 1,000 year) time scales [8,10,13,14]. Previous analyses of global carbon burial in the oceans neglected the role of turbidity currents, assuming that terrestrial organic carbon supplied by rivers was buried almost exclusively within deltas or continental shelves [11,12]. Past studies also inferred most terrestrial organic carbon was remineralised on continental shelves, as occurs offshore from the Amazon River [11,12, 75], such that the global burial efficiency of terrestrial organic carbon in marine sediments was low (10-44%) [11-13]. However, recent work suggested terrestrial organic burial by turbidity currents can be highly efficient (>60-100%) in a wide range of settings 8,14]. They include the exceptionally large Bengal Fan (Fig. 2d) [8], as well as fjords [76] and systems fed by small mountainous rivers in Oceania [9]. This recently led to revised global estimates for mass-flux (~62-90 Mt C/yr) and efficiency (31-45%) of terrestrial OC burial in marine sediments [14]. Photosynthesis in the surface ocean produces a far greater (50,000 MtC/yr) amount of organic carbon [77], but only 90-130 MtC/yr of that marine carbon is buried at the seabed (Fig. 2b) [10-14,77]. Thus, burial flux of terrestrial organic carbon from turbidity currents approaches that due to settling from the surface ocean [14], although only marine carbon produced via photosynthesis in the surface ocean will affect atmospheric pCO_2 and thus climate on shorter term (<100 yr) time scales (Fig. 2c) [78].

Almost all rivers would connect directly to submarine canyons during glacial low-stands [67,68], so that global burial flux of terrestrial organic carbon will likely increase to >60-80% [14]. This raises the possibility that terrestrial organic carbon burial by turbidity currents varies systematically and substantially through glacial-interglacial cycles [79]. It is often inferred that changes in surface ocean productivity further reduced atmospheric pCO_2 levels during glacial periods [e.g. 78]. But more efficient terrestrial organic carbon burial by turbidity currents could also have acted as a positive feedback to reduce atmospheric pCO_2 levels during glacials, albeit over much longer (> 1,000 years) timescales [79]. Thus, the magnitude of change in organic carbon burial flux via turbidity currents between glacial and inter-glacial periods (~30-95 Mt/yr) can rival changes in global organic carbon burial proposed to drive other longer-term climate fluctuations [14]. For example, Li et al. [80]

inferred comparable changes in global organic carbon burial flux (~90 Mt/yr) were an important positive feedback for global warming during the Neogene.

A more active turbidity current carbon pump may also have significant implications for seabed life, as organic carbon underpins most marine food webs [81]. Turbidity currents also physically disturb ecosystems by scouring the seabed, sometimes to depths of tens of meters, or by depositing thick sediment layers that smother ecosystems [17]. Rapid accumulation of organic-rich sediment can also lead to chemotrophic ecosystems resembling those around black smokers [82]. Thus, impacts of turbidity currents on marine life warrant further analysis.

Monitoring projects are also showing how human activities may trigger turbidity currents, and thus impact wide areas of the seafloor. For example, it has been shown how bottom trawling can both smooth (plough) the seabed, and initiate turbidity currents that travel down canyons [18]. This canyon-monitoring work built upon previous remarkably determined efforts to record how cold and dense water masses formed on continental shelves could sometimes cascade down submarine canyons [83]. It took almost a decade of research cruises to record these strong dense water cascades in action, but it showed how direct measurements can lead to major advances [83]. More recently, it is being shown how turbidity currents may disperse microplastic and other pollutants [19], or ventilate the deep ocean with warmer and more oxygenated water [84].

What turbidity currents comprise

There has long been controversy over what turbidity currents comprise [1,26,86-86]. This debate centres on whether they are entirely dilute and fully turbulent sediment suspensions, as for most rivers, or driven by dense near-bed layers that resemble debris flows [86]. This debate is not just in the detail; it is critical because the basic physics of dense or dilute sediment flows are very different, and there is a need to know what type of flow to model in the laboratory or numerically [86]. Geologists tried to answer this question by examining turbidite deposits, but the answer is often ambiguous, especially when deposits comprise massive or planar laminated sand (i.e. Bouma sequence divisions T_A and T_B) [86].

Detailed measurements from within turbidity currents thus play a key role in understanding their internal nature (Fig. 6). They show the velocity structure of turbidity currents can differ significantly from laboratory experiments, where a faster-moving body feeds a slower-moving head (Fig. 6b) [33]. Measurements from the Congo Canyon show that turbidity currents instead comprise a fast-moving frontal zone ('frontal cell') that outruns a much slower-moving body, leading to flow stretching [36,37] (Fig. 6a,b). Such stretching might explain the surprising week-long duration of Congo Canyon flows (Fig. 6a). Elsewhere, sand-dominated turbidity currents also displayed a short-lived (< 30 min) frontal cell where velocities are fastest (Fig. 6c), but these flows only lasted for minutes to hours (Fig. 6c; Supplementary Fig. 1d) [34,35,41,45,46,50,53]. They lacked the sustained week-long body seen in Congo Canyon flows (Fig. 5a), presumably because Congo Canyon flows contain more mud that settles slowly [36,37].

There is also mounting evidence that faster (>1.5 m/s) turbidity currents contain denser near-bed layers at their front, which drive the flow (Fig. 6) [35,38,40]. Multibeam echosounders imaged denser near-bed layers at Squamish Delta (Canada) [38], but only in fast-moving (>1.5 m/s) flows, although their exact sediment concentration is unknown. Transit (flow front) velocities in Monterey Canyon were quicker than maximum velocities measured by ADCPs (acoustic Doppler current profilers) inside the flow [35]. This was initially puzzling, as the flow front must push through surrounding seawater that retards its progress. But ADCPs typically do not measure within a few meters of the bed, and this suggest the presence of a thin and fast layer near the bed [35]. Even more surprisingly, very heavy (up to 800 kg), dense (up to 6 g/cm^3) and irregularly shaped objects (Fig. 4f) were carried for several kilometres down Monterey Canyon at speeds of up to 4 m/s, comparable to maximum flow speeds [35, 52]. These objects had different mass, densities and shapes, yet sometimes moved together in lock step [35, 52]. Dense near-bed layers appear to have entombed and rafted the heavy objects (Fig. 4f), and this is supported by a conductivity probe that dipped close to the bed to record sediment volume concentrations of >11% [49]. Pope et al. [40] then used an equation that predicts vertically-averaged sediment concentrations using independently measured flow velocities and thicknesses, and a friction coefficient (Fig. 6c-e). This Chezy-equation was applied to turbidity currents in Bute Inlet (Canada) to show that fast (>1.5 m/s) flows were relatively dense (> ~10% and up to 38% sediment volume; Fig. 6c), whilst slower moving flows were entirely dilute (Fig. 6e; [40]). The dense parts of flows carry most of the sediment and drive the overall event [40], and they are likely characterised by strongly damped turbulence and hindered settling, as well as grain-to-grain interactions.

Additional strong evidence shows that slower moving flows are entirely dilute (Fig. 6e). For example, acoustic backscatter measurements from ADCPs can be used to derive sediment concentrations, after making some assumptions about grain sizes [36, 37]. This method concludes that the overlying sediment cloud and trailing body (Fig. 6a) typically has sediment concentrations of just 0.1 to 0.001% by volume in the Congo Canyon [37].

Field evidence also supports a view that flows may evolve from having a dense near-bed layer to become entirely dilute and fully turbulent as they decelerate [35,40]. For example, dense near-bed layers were not observed by multibeam sonars in slower flows at Squamish Delta [38], and objects were not carried for such long distances at more distal sites in Monterey Canyon [35]. Pope et al. [40] used the Chezy-equation to show how flows evolved from having a dense frontal layer to being entirely dilute as they decelerated (Fig. 6c-e).

Behaviour of turbidity currents

Submarine turbidity currents have been compared to terrestrial river systems, such as in the way they produce meandering channels, but their behaviour differs in some fundamental regards [24]. Unlike rivers, turbidity currents are driven by the weight of sediment they carry, and density differences with surrounding seawater. Turbidity currents that erode the seabed can therefore become denser and faster, causing even more erosion and acceleration, producing a positive feedback termed ‘ignition’ (Fig. 7b) [25]. Alternatively, erosion and deposition of sediment may be balanced, such that turbidity currents maintain a uniform velocity and near equilibrium state (Fig. 7c) [4, 25]. Finally, deposition of sediment will reduce flow densities and thus velocity, leading to further sediment settling, such that flows dissipate (Fig. 7a).

Direct monitoring measurements can now test these basic hypotheses for how turbidity currents behave. Detailed information on spatial changes in flow front speed is only available from a handful of sites, but these datasets show a remarkably consistent pattern (Fig. 7d) [4,40,87]. Flow behaviour tends to bifurcate, depending on initial velocities (Fig. 7d). Initially faster-moving flows (>4-5 m/s) sustain near-uniform front velocities or gradually accelerate, and thus runout much further [4,87]. Flows that initially travel at slower speeds die out over much shorter distances (Fig. 7d) [4,87]. It is not yet clear why some flows (but not others) reach these higher initial speeds, but it could result from initial remobilisation of larger volumes of sediment, which then produces thicker and denser flows.

Three further key insights emerge from comparison of changes in flow speeds at different sites (Fig. 7d). First, previous theory predicts sediment grain size and settling velocity should have a strong impact on the threshold flow speed needed for either ignition or autosuspension [25]. However, a similar threshold speed (4-5 m/s) occurs in sand-dominated (Monterey Canyon) and mud-dominated (Congo Canyon) settings (Fig. 7d) [4,87]. The critical initial speed needed for ignition or autosuspension therefore appears to be independent of the settling velocity of individual grains, perhaps because faster flows have dense near-bed layers where grains interact and do not settle individually. Second, although initial front speeds are a good predictor of ignition-autosuspension, they are a poor predictor of runout distance, or depth and volume of erosion. For example, flows with speeds of 5-8 m/s in Congo Canyon ran out for > 1,100 km, and eroded a huge sediment volume, equivalent to 19-35% of the annual flux from all rivers [4], whilst flows travelling initially at similar speeds in Monterey Canyon ran out for >50 km, and caused little net erosion of the seabed (Fig. 7d) [35,52,87]. Third, although ignition may occur, it occurs gradually over long distances, and many flows tend towards a near-uniform front speed (Fig. 7d). Indeed, flows in the Congo Canyon combine elements of ignition (erosion of the seabed) and elements of autosuspension (near uniform flow front speeds) [4].

This has led to a new ‘travelling wave’ model (Fig. 7e) for how turbidity currents evolve, in which flows may be highly erosive (as for ignition) yet maintain near uniform speeds (as for autosuspension) [4,87]. In this model, the event is driven by a dense, partially liquefied, near-bed layer (travelling wave) at its front [4,87]. Erosion at the base of the dense layer, is balanced by sediment deposition or transfer into a trailing dilute sediment cloud, leading to near-uniform speeds (Fig. 7e). However, this model may not hold in unconfined settings, such as basin plains, where very long (up to 2,000 km) runouts on low gradients (0.05°) can occur without significant seabed erosion [86,88]. In such settings, slow settling cohesive mud may provide the flow’s main driving force. Indeed, mud may form vast fluid-mud layers that only come to a halt and pond in bathymetric lows at the far end of deep-sea basins [86,89].

Observations in Monterey Canyon also point to the importance of seabed properties and processes of sediment entrainment for turbidity current behaviour [87]. One of 16 flows monitored in 2016-18 accelerated within the mid-canyon, and this was the only flow to occur in summer months [87]. It seems most likely that this summer event either entrained a seasonally developed weak mud-layer, or triggered local failure of the seabed, thereby causing anomalous mid-canyon acceleration [87]. Time-lapse mapping of the Congo Canyon also shows erosion of the seabed may be extremely patchy and localised on the canyon floor, even where flows speeds remain relatively uniform [4,5]. Local areas of deep (20-30 m) erosion are associated with waterfall-like features called knickpoints (Fig. 6). Indeed, cable break observations worldwide show sequences of cables breaking and surviving, suggesting uneven seabed erosion may be ubiquitous [4-6, 90]. It is not inevitable that a fast turbidity current will break a cable. Cables that break may be located close to knickpoints, whereas cables that survive are located away from knickpoints [4,5]. This could be tested by further time-lapse mapping. Understanding and predicting rates of seabed erosion are a remaining grand challenge, and it is critical for flow modelling, as patterns of erosion or deposition may control flow behaviour [91].

How turbidity currents sculpt the seabed

Repeat (time lapse) mapping of the seabed is also providing major new insights into how turbidity currents interact with the seabed [4, 17, 35, 38, 39, 43, 52, 57, 48, 54, 59, 92, 93]. It is also showing how turbidity currents may differ in key regards from terrestrial rivers [25]. For example, flows exist in one of two basic states; supercritical flow is thinner and faster, whilst subcritical flow is slower and thicker. A critical Froude number (Fr) separates supercritical (Fr > 1) from subcritical (Fr < 1) flow, with this Froude number being proportional to flow speed and inversely proportional to the density contrast between flow and surrounding medium [94-97]. Subcritical flow occurs in most terrestrial rivers and produces bedforms such as dunes and ripples that migrate down-slope. However, turbidity currents are more prone to supercritical flow than rivers, due to their lower density contrast with surrounding seawater, and often faster speeds [94-97]. There is indeed mounting evidence that supercritical turbidity currents are widespread on the seafloor [98]. Spectacular trains of up-slope migrating bedforms have been mapped on submarine canyon floors worldwide [35,38,39], on open continental slopes [98], and flanks of volcanoes [99]. Combined flow monitoring and time-lapse seabed mapping has shown how these up-slope migrating bedforms are linked to instabilities in supercritical flows [38,50], termed cyclic steps, which lead to repeated alternations of supercritical and subcritical flow separated by hydraulic jumps [94-97].

Time-lapse mapping is also showing how up-slope migrating knickpoints that are 10-30 m high may dominate submarine channel-bend evolution (Supplementary Figure 2) [92]. Knickpoints can occur in river channels. However, their submarine cousins can be much faster moving and migrate for hundreds of meters or more each year, driven by overpassing turbidity currents [92, 93]. Knickpoints in rivers are caused by external processes such as fault-uplift, sea-level variation and changes in bedrock, but this is not normally the case for submarine knickpoints that are formed by internal processes such as cyclic steps or seabed loading and failure [92]. These seabed knickpoints excavate submarine channels, whilst depositing sediment in adjacent downstream areas (Supplementary Fig. 2) [92]. Knickpoints also play a key role in how sediment, organic carbon and pollutants may be shuffled in multiple stages to the deep-sea [100].

In meandering rivers, secondary (across-channel) flow at bends tends to sweep sediment towards the inner-bank to form point bars [24]. However, vigorous debate has centred on whether the secondary flow in turbidity currents occurs as in rivers, with near-bed flow towards the inner-bank of a bend, or is reversed with near-bed flow towards the outer-bank [24,101,102]. Flow monitoring at a bend in the Congo Canyon suggests that two secondary flow cells occur, with near-bed flow sweeping sediment towards the outer bend [103]. But knickpoint migration may be more important than secondary flow patterns for bend evolution, at least in some settings (Supplementary Fig. 2) [92,100].

Turbidity currents were first proposed to explain the origin of huge underwater canyons that were discovered in the 1800s on ocean and lake floors [1,104,105]. Available time-lapse mapping currently only extends for a few decades at most [92,106], but it is starting to help understand how these canyons form. For example, time-lapse mapping of the Kaikōura Canyon offshore Aotearoa New Zealand, before and after a major (M_w 7.8) earthquake in 2016, shows how the earthquake caused widespread failure of the canyon-rim and other areas [17]. This produced a turbidity current that caused gravel waves to move down-canyon and eroded > 1 km^3 of sediment, a volume that is 2-3 times the sediment entering the ocean annually from Aotearoa rivers. This flow swept seabed life from a canyon that had one of the highest benthic biomasses on Earth, and carried ~7 Mt of particulate organic carbon to the deep-sea [17]. Time-lapse mapping of the Congo Canyon revealed that turbidity currents eroded ~2.6 km^3 of sediment in just one year, and flushed this sediment and associated organic carbon into the deep-sea [4]. These repeat surveys show how fresh organic carbon from river floods may be fast-tracked by turbidity currents, and explain how organic carbon burial by turbidity currents may be highly efficient (Fig. 2b,d; Fig. 3) [8]. Time-lapse studies have also showed how canyon-flank collapse may produce landslide-dams with implications for sediment and organic carbon transfer. A ∼0.09 km^3 canyon-flank landslide dammed the Congo Canyon, causing temporary storage of a further ∼0.4 km^3 of sediment with ∼5 Mt of (mainly terrestrial) organic carbon [106]. The trapped sediment was up to 150 m thick, and extended >26 km up-canyon of the landslide-dam, and this dammed sediment is currently being eroded and gradually released [106].

Meter-scale resolution seabed surveys are being collected using autonomous underwater vehicles (AUVs) that fly at just a few tens of meters above the seabed, providing major new insights into how submarine channel and fan systems operate [35, 43, 52, 107-110]. Previous influential models of such systems assumed that channels bifurcated down-slope at their termination, to form a distributary network, in the same way that many rivers bifurcate to create deltas [111]. However, AUV mapping of submarine channel mouth terminations now show that only a single main channel is active, although there may be fields of scours and bedforms, as well as adjacent headless channels that fail to connect to the main channel [109]. This channel mouth geomorphology is radically different to that seen in laboratory experiments [112], and its significance for flow processes remains poorly understood.

Understanding how deposits are formed

Ancient turbidity current deposits (turbidites) form rock sequences in numerous locations worldwide, which can be kilometers thick, and accumulate over thousands to millions of years [111,113]. Geologists have proposed models for how flows and deposits are linked, based on this rock record, but such models are difficult to test without observing the flow itself [86]. Direct measurements from active flows are thus now being combined with analysis of seabed cores to directly show how parent flows are recorded by their deposits. These studies are producing major new insights, albeit only for processes operating over rather short (days to a few years) time-scales, rather than longer term processes occurring over thousands of years.

For example, seabed cores were combined with time-lapse mapping and direct flow measurements to show how trains of cyclic step bedforms created by supercritical flows [38] are recorded in deposits [50]. It showed how individual flow deposits comprising mainly massive sand are linked to dense near-bed layers. Up-slope migration of single bedforms initially produced backstepping stratal geometries, yet they were then eroded by migration of subsequent bedforms with complex and offset crests to leave complex nested scours [50,114].

Time lapse mapping has also been used to understand completeness of turbidite deposits, and how much of initially deposited sediment is finally preserved in the rock record. For example, ~90 near-daily surveys spanning ~3 months [38] mapped patterns of erosion and deposition offshore Squamish Delta [115]. They show that only 11% of sediment originally deposited within channels was preserved, even on these very short (3 month) time scales [115]. Seabed cores in Monterey Canyon were combined with direct flow measurements, as well as moored traps that captured sediment from within the flow [51,81,98]. This work showed sand can be restricted to a few meters above the canyon floor, and internal tides occurring between turbidity currents stir up fine-mud, so that the fine-mud is poorly recorded in sand-dominated canyon floor cores [51]. Organic carbon may also be kept in suspension, such that it is underrepresented in seabed cores [81].

A puzzling feature of individual ancient turbidite beds is that they have a distinctly bimodal distribution of thickness and internal deposit types [116]. Thicker (>40 cm) beds tend to contain intervals of massive and planar laminated sand, whilst thin beds (<40 cm) tend to comprise only ripple cross-laminated sand and overlying mud [116]. Long distance mapping of individual turbidite deposits shows how flows may evolve from thick to thin beds, with a relatively sharp termination of massive and planar-laminated intervals [86,117]. Direct monitoring may now explain why turbidite deposits are bimodal [40]; faster flows contain a dense near-bed layer that can deposit massive and planar-laminated sand, whilst slower flows are entirely dilute and produce thinner turbidite deposits with cross-bedding (Fig. 6c,e) [40].

Future directions

There are now exciting opportunities to use direct monitoring data from turbidity currents to test computational or analytical flow models, design more realistic laboratory flume experiments, or understand deposits. Models and flume experiments need to simulate near-bed layers with high (10-30%) sediment concentrations in faster (> ~1.5 m/s) flows. A key challenge is to develop a robust theoretical framework for how such hyper-concentrated layers behave, in which turbulence is damped strongly, grain settling is hindered, yet deposition occurs incrementally rather than en-masse. This framework would be comparable to that developed recently for even higher sediment concentration debris flows by Iverson and others [119], where en-masse deposition occurs.

This review is also a rally call for widespread global monitoring of turbidity currents, over longer timescales, and underpinned by a new generation of sensors that are deployed at significantly lower cost and risk. The current situation is broadly comparable to trying to understand how rivers work globally, using sporadic and incomplete monitoring from just ~10 sites, mainly smaller streams. We need to study locations where occurrence of turbidity currents would be more surprising, as shown by work in Whittard Canyon (Supplementary Figure 1) [69], or other types of system such as those with hyperpycnal flows.

A key issue is that moored sensors tend to be broken by faster (> 5m/s) turbidity currents [4, 118], such that other types of sensors are needed that can be placed outside the active flow, and thus out of harm's way. Seismic signals (ground shaking) [120] or acoustic noise [121] emitted by turbidity currents may underpin a new generation of sensors that remotely sense turbidity currents from a safe distance. Indeed, an exciting development is that submarine landslides may also be remotely sensed using seismic signals, at low cost, simultaneously over large ocean basins. Fan et al. [122] use such signals to infer that 75 of the 85 landslides that occurred in a 7-year period in the Gulf of Mexico were triggered by remote and sometimes moderate earthquakes, which were hundreds or even thousands of kilometers away [122]. Lower cost sensing systems are also needed that relay data back to base via surface floats and satellites, rather than being retrieved by expensive vessels [118]. Without these lower cost systems, we will only ever have funds to study just a few sites.

Currently, direct monitoring is good at measuring flow velocities (Fig. 6); yet the most important parameter may be the flow's sediment concentration and density, as this is what drives the flow [1], and determines sediment mass-flux. Future monitoring studies need to focus on how to measure sediment concentration in turbidity currents, as well as how flows erode the seabed, as mass-exchange with the bed often dominates overall flow behaviour [91]. Methods to constrain mass fluxes, together with a more global monitoring network, could then answer a remaining grand scientific challenge. This is to determine the global sediment and organic carbon fluxes carried by turbidity currents, and their fundamental controls, and therefore how these fluxes compare to other major global sediment and carbon pumps on Earth (Fig. 2a-c).

References

[1] Kuenen, P.H. and Migliorini, C.I. Turbidity currents as a cause of graded bedding. J. *Geol.* **58**, 91–127 (1950).

[2] Heezen B.C. & Ewing, M**.** Turbidity currents and submarine slumps, and the 1929 Grand Banks earthquake. *Am. J. Science*, **250**, 849-873 (1952).

[3] Piper, D.J.W., Cochonat, P. & Morrison M.L. The sequence of events around the epicenter of the 1929 Grand Banks earthquake: initiation of the debris flows and turbidity current inferred from side scan sonar. *Sedimentology,* **46**, 79-97 (1999).

[4] Talling, P.J. et al.. Longest sediment flows yet measured show how major rivers connect efficiently to deep-sea. *Nature Comms*, **13,** 4193 (2022).

[5] Talling, P.J. et al.. Flood and tides trigger longest measured sediment flow that accelerates for thousand kilometers into deep-sea. A white paper on submarine cable geohazards archived on Earthxiv. doi.org/10.31223/X5W328 (2022).

[6] Carter, L., Milliman, J., Talling, P.J., Gavey, R., & Wynn, R.B. Near-synchronous and delayed initiation of long run-out submarine sediment flows from a record breaking river-flood, offshore Taiwan. *Geophys. Res. Lett.* **39**, L12063 (2012).

[7] Carter, L., Gavey, R., Talling, P. & Liu, J. Insights into submarine geohazards from breaks in Subsea Telecommunication Cables. *Oceanography* **27**, 58–67 (2014).

[8] Galy, V. et al. Efficient organic carbon burial in the Bengal fan sustained by the Himalayan erosional system. *Nature* **450**, 407-410 (2007).

[9] Kao, S-J. et al. Preservation of terrestrial organic carbon in marine sediments offshore Taiwan: mountain building and atmospheric carbon dioxide sequestration. *Earth Surf. Dynam*. **2**, 127–139 (2014).

[10] Hilton, R.G. & West, A.J. Mountains, erosion and the carbon cycle. *Nature Reviews, Earth & Environment* **1**, 284–299 (2020).

[11] Berner, R.A. 1989. Biogeochemical cycles of carbon and sulfur and their effect on atmospheric oxygen over Phanerozoic time. *Palaeogeogr. Palaeoclimatol. Palaeoecol.* 73, 97–122.

[12] Burdige, D.J. Burial of terrestrial organic matter in marine sediments: a reassessment. *Glob. Biog. Cycles* **19**, GB4011 (2005).

[13] Blair, N.L. & Aller, R.C. 2012. The fate of terrestrial organic carbon in the marine environment. *Annual Rev. Marine Sci.* **4**, 401–423.

[14] Talling, P.J., Hage, S., Baker, M.L., Bianchi, T.S., Hilton R.G., & Maier, K.L. The global turbidity current pump and its implications for organic carbon cycling. Ann. Revs. Marine Sci. in press (2023).

[15] Amaro, T. et al. The Whittard Canyon – A case study of submarine canyon processes. *Progress in Oceanography* **146** (2016) 38–57.

[16] Rabouille, C., Baudin, F., Dennielou, B. & Olu, K. Organic carbon transfer and ecosystem functioning in the terminal lobes of the Congo deep-sea fan: outcomes of the Congolobe project. *Deep-sea Res. Part II* **142**, 1–6 (2017).

[17] Mountjoy, J.J. et al. Earthquakes drive large-scale submarine canyon development and sediment supply to deep-ocean basins. *Sci. Adv*. **4**, eaar3748 (2018).

[18] Puig, P. et al. Ploughing the deep-sea floor. *Nature* **489**, 286–289 (2012).

[19] Kane, I.A. & Clare, M.A. Dispersion, accumulation, and the ultimate fate of microplastics in deep-marine environments: a review and future directions. Frontiers in Earth Science 7, article 80 (2019).

[20] Goldfinger, C. Submarine paleoseismology based on turbidite records. *Annual Review of Marine Science* **3**, 35-66 (2011).

[21] Howarth, J.D. et al. Calibrating the marine turbidite paleoseismometer using the 2016 Kaikōura earthquake. *Nature Geosci.* **14,** 161–167 (2021).

[22] Talling, P.J. Fidelity of turbidites as earthquake records. *Nature Geosci.* **14**, 113–116 (2021).

[23] Pettingill, H.S. &Weimer, P. Worldwide deepwater exploration and production: Past, present, and future. *Leading Edge* **21**, 371 (2002).

[24] Peakall, J., & Sumner, E.J. Submarine channel flow processes and deposits: A process-product perspective. Geomorphology 244, 95–120 (2015).

[25] Parker, G., Fukushima, Y. & Pantin, H.M. Self-accelerating turbidity currents. *J. Fluid Mech.*, **171**, 145-181 **(**1986).

[26] Lowe, D.R. Sediment gravity flows. 2. Depositional models with special reference to high density turbidity currents. *J. Sedim. Petrol.*, **52**, 279-298 (1982).
[27] Inman, D.L., Nordstrom, C.E., & Reinhard, E.F. Currents in submarine canyons: an air–sea–land interaction. *Ann. Rev. Fluid Mech* **8,** 275–310 (1976).
[28] Dill, R.F. Earthquake effects on fill of Scripps Submarine Canyon. *Geol. Soc. Am. Bull.* **80**, 321–328 (1969).
[29] Hay, A.E., Burling, E.W., & Murray, J.W. Remote acoustic detection of a turbidity current surge. *Science* **217**, 833–845 (1982).
[30] Bornhold, B.D., Ren, P., & Prior, D.B. High-frequency turbidity currents in British Colombia fjords. *Geo-Mar. Letts* **14**, 238–243 (1994).
[31] Khripounoff, A. et al. Direct observation of intense turbidity current activity in the Zaire submarine valley at 4000 m water depth. *Marine Geol.* **194**, 151–158 (2003).
[32] Talling, P.J. et al. Key future directions for research on turbidity currents and their deposits. *J. Sedim. Res.* **85,** 153-169 (2015).
[33] Kneller, B., & Buckee, C. The structure and fluid mechanics of turbidity currents: a review of some recent studies and their geological implications. *Sedimentology* **47**, 62-94 (2002).
[34] Xu, J. P., Noble, M. A., & Rosenfeld, L. K. In-situ measurements of velocity structure within turbidity currents. *Geophys. Res. Lett*., **31**, L09311 (2004).
[35] Paull, C.K. et al. Powerful turbidity currents driven by dense basal layers. *Nature Communications* **9**, 4114 (2018).
[36] Azpiroz-Zabala, M. et al. Newly recognized turbidity current structure can explain prolonged flushing of submarine canyons. *Sci. Advances* **3**, e1700200 (2017).
[37] Simmons, S.M. et al. Novel acoustic method provides first detailed measurements of sediment concentration structure within submarine turbidity currents. *J. Geophy. Res*. **125**, e2019JC015904.
[38] Hughes Clarke, J.E. First wide-angle view of channelized turbidity currents links migrating cyclic steps to flow characteristics. *Nature Comms* 7, 11896 (2016).
[39] Hage, S. et al. Direct monitoring reveals initiation of turbidity currents from extremely dilute river plumes. *Geophy. Res. Letts* **46**, 11,310 - 11,320 (2019).
[40] Pope, E.L. et al. First source-to-sink monitoring shows dense head determines sediment gravity flow runout. Science Advances, 8, eabj3220 (2022).

[41] Liu, J.T., Kao, S.-J., Huh, C.-A., & Hung, C.-C. Gravity flows associated with flood events and carbon burial: Taiwan as instructional source area. *Ann. Revs. Marine Science* **5**, 47–68 (2013).
[42] Liu, J.T. et al. Cyclone induced hyperpycnal turbidity currents in a submarine canyon. *J. Geophys. Res.* **117**, C04033 (2012).
[43] Normandeau, A. et al. Storm-induced turbidity currents on a sediment-starved shelf: Insight from direct monitoring and repeat seabed mapping of upslope migrating bedforms. *Sedimentology* ***67,*** 1045–1068 (2020).
[44] Xu, J.P., Swarzenski, P.W., Noble, M., & Li, A.-C. Event-driven sediment flux in Hueneme and Mugu submarine canyons, Southern California. Marine Geology 269, 74–88 (2010).
[45] Khripounoff, A., Crassous, P., Lo Bue, N., Dennielou, B., & Silva Jacinto, R. Different types of sediment gravity flows detected in the Var submarine canyon (northwestern Mediterranean Sea): *Prog. Oceanography* **106**, 138–153 (2012).
[46] Heerema, K. et al. How distinctive are flood-triggered turbidity currents? *J. Sedim. Res.* **92**, 1–11 (2022).
[47] Lintern, D.G., Hill, P.R. & Stacey, C. Powerful unconfined turbidity current captured by cabled observatory on the Fraser River delta slope, British Columbia, Canada. *Sedimentology* **63**, 1041–1064 (2016).
[48] Hill, P.R. & Lintern, D.G. Turbidity currents on the open slope of the Fraser Delta. *Marine Geology* **445**, 106738 (2022).
[49] Wang, Z. et al. Direct evidence of a high-concentration basal layer in a submarine turbidity current. *Deep-sea Res. Part I* **161**, 103300 (2020).
[50] Hage, S. et al. How to recognize crescentic bedforms formed by supercritical turbidity currents in the rock record: insights from active submarine channels. *Geology* **6**, 563-566 (2018).
[51] Maier, K.L. et al. Linking direct measurements of turbidity currents to submarine canyon-floor deposits. *Front. Earth Sci. (Sedimentology, Stratigraphy and Diagenesis)*. doi: 10.3389/feart.2019.00144 (2019).
[52] Meng, L., Wang, Z., & Xu, J. Two distinct types of turbidity currents observed in the Manila Trench, South China Sea. *Commun Earth Environ* **4**, 108 (2023).
[53] Gwiazda, R. et al. Near-bed structure of sediment gravity flows measured by motion-sensing 'boulder-like' Benthic Event Detectors (BEDs) in Monterey Canyon. *J. Geophys. Res*. 127 (2022).

[54] Hill, P. Changes in submarine channel morphology and slope sedimentation patterns from repeat multibeam surveys in the Fraser River delta, western Canada. *Int. Assoc. Sedimentol. Spec. Pub.* **44**, 47–70 (2012).
[55] Talling, P.J., Paull, C.K. & Piper, D.J.W. How are subaqueous sediment density flows triggered, what is their internal structure and how does it evolve? Direct observations from monitoring of active flows. *Earth Sci. Revs* **125**, 244-287 (2014).
[56] Piper, D.J.W. & Normark, W.R. Processes that initiate turbidity currents and their influence on turbidites: a marine geology perspective. *J. Sedim. Res.* **79**, 347–362 (2009).
[57] Clare, M.A. et al. Direct monitoring of active geohazards: emerging geophysical tools for deep-water assessments. *Near Surf. Geophys* **15**, 427-444 (2017).
[58] Mulder, T., Syvitski, J.P.M., Migneon, S., Faugeres, J.C. & Savoye, B. Marine hyperpycnal flows: initiation, behaviour, and related deposits. A review. *Mar. Petrol. Geol.*, **20**, 861-882 (2003).
[59] Hizzett, J. L. et al. Which triggers produce the most erosive, frequent and longest runout turbidity currents on deltas? *Geophys. Res. Letts* **45**, 855-863 (2017).
[60] Bailey, L.P. et al. Preconditioning by sediment accumulation can produce powerful turbidity currents without major external triggers. *Earth & Planetary Sci. Letts* **562**, art.116845 (2021).
[61] Clare, M.A., Hughes Clarke, J.E., Talling, P.J., Cartigny, M.J. & Pratomo, D.G. Preconditioning and triggering of offshore slope failures and turbidity currents revealed by most detailed monitoring yet at a fjord-head delta. *Earth & Planet. Sci. Letts* **450**, 208-220 (2016).
[62] Sawyer, D. & DeVore, J. Evidence for seismic strengthening from undrained shear strength measurements. *Geophys. Res. Letts* **42**, 10,216-10,221(2016).
[63] McHugh, C.M. et al. Remobilization of surficial slope sediment triggered by the A.D. 2011 M_w9 Tohoku- Oki earthquake and tsunami along the Japan Trench. *Geology* **44**, 391–394 (2016).
[64] Moernaut, J. et al. Lacustrine turbidites as a tool for quantitative earthquake reconstruction: New evidence for a variable rupture mode in south central Chile. *J. Geophys. Res.* **119**, 1607–1633 (2014).
[65] Hunt, J.E., Wynn, R.B., Masson, D.G., Talling, P.J., & Teagle, D.A. Sedimentological and geochemical evidence for multistage failure of volcanic island landslides: a case study from Icod landslide on north Tenerife, Canary Islands. *G-cubed*, GC003740 (2011).

[66] Posamentier, H.W., Erksine, R.D. & Mitchum, R.M., Jr. Submarine fan deposition within a sequence stratigraphic framework, in Welmer, B., and Link, M.H., eds., Seismic facies and sedimentary processes of submarine fans and turbidite systems: New York, Springer Verlag, 127–136 (1991).
[67] Harris, P. T. & Whiteway, T. Global distribution of large submarine canyons: Geomorphic differences between active and passive continental margins. *Mar. Geol.* **285,** 69–86 (2011).
[68] Bernhardt, A. & Schwanghart, W. Where and why do submarine canyons remain connected to the shore during sea-level rise? Insights from global topographic analysis and Bayesian regression. *Geophys. Res. Lett*. **48**, e2020GL092234 (2021).
[69] Heijnen, M.S. et al. Challenging the highstand-dormant paradigm for land-detached submarine canyons. *Nature Comms* **13**, 3448 (2022).
[70] Covault, J. A. & Graham, S. A. Submarine fans at all sea-level stands: Tectono-morphologic and climatic controls on terrigenous sediment delivery to the deep-sea. *Geology* **38**, 939-942 (2010).
[71] Milliman, J. D. & Farnsworth, K. L. River discharge to the coastal ocean: a global synthesis, Cambridge University Press (2011).
[72] Rogers, K.G., Goodbred Jr., S.L. & Khan, S.R. Shelf-to-canyon connections: Transport-related morphology and mass balance at the shallow-headed, rapidly aggrading Swatch of No Ground (Bay of Bengal). *Marine Geology* **369**, 288–299 (2015).
[73] Wright, L.D., Friedrichs, C.T., Kim, S.C., & Scully, M.E. Effects of ambient currents and waves on gravity-driven sediment transport on continental shelves. *Marine Geol.* **175**, 25–45 (2001).
[74] Wheatcroft, R.A., & Sommerfield, C.K. River sediment flux and shelf sediment accumulation rates on the Pacific Northwest margin. *Cont. Shelf Res.* **25**, 311–332 (2005).
[75] Aller, R.C. & Blair, N.E. Carbon remineralization in the Amazon–Guianas mobile mudbelt: a sedimentary incinerator. *Cont. Shelf Res.* **26**, 2241–2259 (2006).
[76] Smith, R., Bianchi, T., Allison, M., Savage, C. High rates of organic carbon burial in fjord sediments globally. *Nature Geosci*. **8**, 450–453 (2015).
[77] Dunne, J.P., Darmiento, J.L. & Gnanadesikan, A. Synthesis of global particle export from the surface ocean and cycling through ocean interior and on the seafloor. *Glob. Biog. Cycl*. 21, GB4006 (2007).
[78] Sundquist, E.T. The global carbon-dioxide budget. *Science* **259**, 934-941.

[79] Cartapanis, O., Galbraith, E.D., Bianchi, D. & Jacard, S.L. Carbon burial in deep-sea sediment and implications for oceanic inventories of carbon and alkalinity over the last glacial cycle. *Clim. Past.* **14**, 1819–1850 (2018)
[80] Li, Z., Zhang, Y.G., Torres, M., Mills, B.J.W. Neogene burial of organic carbon in the global ocean. *Nature* **613**, 90-95 (2023).
[81] Maier, K.L. et al. Sediment and organic carbon transport and deposition driven by internal tides along Monterey Canyon, offshore California. *Deep-sea Res.* **153**, 103108 (2019).
[82] Karine, O., Decker, C., Pastor, L., Caprais, J-C., Khripounoff, A., Morioneaux, M., Ain, B., Menot, L., & Rabouille, C. Cold-seep-like macrofaunal communities in organic- and sulfide-rich sediments of the Congo deep-sea fan. *Deep Sea Res.* **142**, 180-196 (2017)
[83] Canals, M. et al. Flushing submarine canyons. Nature 444, 354–357 (2006).
[84] Kao, S.J. et al. 2010, Cyclone driven deep-sea injection of freshwater and heat by hyperpycnal flow in the subtropics. *Geophys. Res. Letts* **37**, L21702.
[85] Shanmugam, G. and R.J. Moiola. Reinterpretation of depositional processes in a classic flysch sequence (Pennsylvanian Jackfork Group), Ouachita Mountains, Arkansas and Oklahoma. *AAPG Bulletin*, **79**, 672-695 (1995).
[86] Talling, P.J., Sumner, E.J., Masson, D.G. & Malgesini, G. Subaqueous sediment density flows: depositional processes and deposit types. *Sedimentology* **59**, 1937-2003 (2012).
[87] Heerema, C.J. et al. What determines the downstream evolution of turbidity currents? *Earth & Planetary Sci. Letts*. **532**, 116023 (2020).
[88] Talling P. J. et al. Onset of submarine debris flow deposition far from original giant landslide. *Nature* **450**, 541-544 (2007).
[89] McCave, I.N. & Jones, K.P.N. Deposition of ungraded muds from high-density non-turbulent turbidity currents. *Nature* **133**, 250-252 (1988).
[90] Gavey, R. et al. Frequent sediment density flows during 2006 to 2015 triggered by competing seismic and weather cycles: observations from subsea cable breaks off southern Taiwan. *Marine Geol.* 384, 147-158 (2017).
[91] Traer, M.M., Hilley, G.E., Fildani, A. & McHargue, T. The sensitivity of turbidity currents to mass and momentum exchanges between these underflows and their surroundings. *J. Geophys. Res.* **117**, F01009 (2012).
[92] Heijnen et al. Rapidly-migrating and internally-generated knickpoints can control submarine channel evolution. *Nature Comms.* **11**, 3129 (2020).

[93] Chen, Y. et al. Knickpoints and crescentic bedform interactions in submarine channels. *Sedimentology* **69**, 1358-1377 (2021).
[94] Kostic, S. & Parker, G. The response of turbidity currents to a canyon-fan transition: hydraulic jumps and depositional signatures. *J. Hydraul. Res*. **44**, 631–653 (2006).
[95] Covault, J.A., Kostic, S., Paull, C.K., Ryan, H.F. & Fildani, A. Submarine channel initiation, filling and maintenance from sea-floor geomorphology and morphodynamic modelling of cyclic steps. *Sedimentology* **61**, 1031–1054 (2014).
[96] Cartigny, M.J.B., Ventra, D., Postma, G. & Van den Berg, J.H. Morphodynamics and sedimentary structures of bedforms under supercritical-flow conditions: new insights from flume experiments. *Sedimentology* **61**, 712–748 (2014).
[97] Slootman, A. & Cartigny, M.J.B. Cyclic steps: Review and aggradation-based classification. *Earth Science Revs.* **201**, 102949 (2020).
[98] Symons, W.O., Sumner, E.J., Talling, P.J., Cartigny, M.J.B., Clare, M.A. Large-scale sediment waves and scours on the modern seafloor and their implications for the prevalence of supercritical flows. *Marine Geology* **371**, 140-178 (2016).
[99] Pope, E.L. et al. Origin of spectacular fields of submarine sediment waves around volcanic islands. E.P.S.L., 493, 12-24 (2018).
[100] Heijnen, M.S. et al. Fill, flush or shuffle: How is sediment carried through submarine channels to build lobes? *Earth & Planet. Sci. Letters* **584**, Art. 117481 (2022).
[101] Corney, R. K. T. et al. The orientation of helical flow in curved channels. *Sedimentology* **53**, 249–257 (2006).
[102] Imran, J. et al. Helical flow couplets in submarine gravity under-flows. *Geology* **35**, 659–662 (2007).
[103] Azpiroz-Zabala, M. et al. A general model for the helical structure of geophysical flows in channel bends. *Geophys. Res. Letts*. 56721 (2017).
[104] Daly, R. A. Origin of submarine "canyons". *American J. Sci.* **31**, 401–420 (1936).
[105] Forel, F-A. Les ravins sous-lacustres des fleuves glaciaires. Comptes rendus de l'académie des sciences de Paris: 1-3 (1885).
[106] Pope, E.L. et al. Landslide-dams affect sediment and carbon fluxes in deep-sea submarine canyons. Nature Geosci. 15, 845–853 (2022).
[107] Maier K.L. et al. Submarine fan development revealed by integrated high-resolution datasets from La Jolla Fan, offshore California. *J. Sedim. Res.* 90, 468–479 (2020).
[108] Paull, C.K. et al. Anatomy of the La Jolla submarine canyon system: offshore southern California. *Marine Geology* **335**, 16-34 (2013).

[109] Hodgson, D.M., Peakall, J. & Maier, K.L. Submarine channel mouth settings: processes, geomorphology, and deposits. *Front. Earth Sci.* 10:790320 (2022).
[110] Wolfson-Schwehr, M., Paull, C.K., Caress, D.W., Gwiazda, R., Nieminski, N.M., Talling, P.J., Carvajal, C., Simmons, S., Troni, G. Time-lapse seafloor surveys reveal how turbidity currents and internal tides in Monterey Canyon interact with the seabed at centimeter-scale. *J. Geophys. Res* **128**, e2022JF006705 (2023).
[111] Mutti, E., Bernoulli, D., Ricci-Lucchi, F., & Tinterri, R. Turbidites and turbidity currents from alpine 'flysch' to the exploration of continental margins. *Sedimentology* **56**, 267-318 (2009).
[112] Baas, J.H., Van Kesteren, W., & Postma, G. Deposits of depletive high-density turbidity currents: a flume analogue of bed geometry, structure and texture. *Sedimentology* **51**, 1053-1088 (2004).
[113] Nielsen T., R.D. Shew, G.S. Steffens & J.R.J. Studlick. Atlas of Deepwater Outcrops, A.A.P.G. Studies in Geology 56, Shell Exploration and Production and A.A.P.G., 504 p (2007).
[114] Englert, R.G. et al. Quantifying the three-dimensional stratigraphic expression of cyclic steps by integrating seafloor and deep-water outcrop observations. *Sedimentology* **68**, 1465–1501 (2021).
[115] Vendettuoli, D. et al. Daily bathymetric surveys document how stratigraphy is built and its extreme incompleteness: One summer offshore Squamish Delta, British Columbia. *Earth & Planet. Sci. Letts* **515**, 231-247 (2019).
[116] Talling, P.J. On the frequency distribution of turbidite thickness: Sedimentology 48, 1297-1329 (2001).
[117] Malgesini, G. et al. Quantitative analysis of submarine-flow deposit shape in the Marnoso-Arenacea Formation: what is the signature of hindered settling from dense near-bed layers? *J. Sedim. Res.* **85**, 170-191 (2015).
[118] Clare, M. et al. Lessons learned from monitoring of turbidity currents and guidance for future platform designs. Geol. Soc. Lond., Spec. Pub. 500, https://doi.org/10.1144/SP500-2019-173 (2020).
[119] Iverson, R.M., Logan, M., LaHusen, R.G., & Berti, M. The perfect debris flow? Aggregated results from 28 large-scale experiments. *J. Geophys. Res.* **115**, F03005 (2010).
[120] Baker, M., Virtual Bouma Conference abstract (2022).
[121] Hay, A.E., Hatcher M. G., & Hughes Clarke, J.E. Underwater noise from submarine turbidity currents. *JASA Express Lett.* 1, 070801 (2021).

[122] Fan, W., McGuire J.J., & Shearer, P.M. Abundant spontaneous and dynamically triggered submarine landslides in the Gulf of Mexico. *Geophys. Res. Letts*. **47**, e2020GL087213 (2020).
[123] Covault, J. A. Submarine fans and canyon-channel systems: A review of processes, products, and models. *Nature Education Knowledge* **3**(10), 4 (2011).
[124] Baudin, F., Rabouille, C., & Dennielou, B. Routing of terrestrial organic matter from the Congo River to the ultimate sink in the abyss: a mass balance approach. *Geologica Belgica* **23/1-2**, 41-52 (2020).
[125] Martin, J., Palanques, A., Vitorino, J., Oliveira, A., & de Stigter, H.C. Near-bottom particulate matter dynamics in the Nazaré submarine canyon under calm and stormy conditions. *Deep-Sea Res. II* **58**, 2388-2400 (2011).
[126] Lambert, A. & Giovanoli, F. Records of riverborne turbidity currents and indications of slope failures in the Rhone delta of Lake Geneva. *Limnol. Oceanog.* **33**, 458-468 (1988).

Acknowledgements

PJT discloses support for the research of this work from the U.K. Natural Environment Research Council (NERC) (grant numbers NE/S010068/1, NE/R001952/1 and NE/K011480/1). KLM acknowledges funding from NIWA Marine Geological Resources Programme and Marsden Grant 21-NIW-014). SH has received funding from the European Union’s Horizon 2020 research and innovation programme under the Marie Sklodowska-Curie grant agreement No 899546. MAC acknowledges funding from the Natural Environment Research Council (NERC) including National Capability Programme (NE/R015953/1) “Climate Linked Atlantic Sector Science” (CLASS), “Environmental Risks to Infrastructure: Identifying and Filling the Gaps” (NE/P005780/1) and “New field-scale calibration of turbidity current impact modelling” (NE/P009190/1).

Contributions

PJT wrote the initial manuscript, with comments from all other authors. All authors played a leading role in collection and analysis of direct flow monitoring data.

Competing Interests

The authors have no competing interests.

Key Points

- It was once thought that submarine turbidity currents were impractical to monitor in action, but detailed monitoring is now possible, and it is revealing major new insights.
- Monitoring identifies new triggers for flows, such as from very dilute river plumes, and consistently shows turbidity currents are much more frequent than predicted by past (e.g. sequence stratigraphic) models.
- Due to turbidity currents, the global burial efficiency of terrestrial organic carbon (28-45%) in marine sediments is significantly higher than previous estimates, and even higher (> 60-80%) during glacial low-stands.
- Faster (> ~1.5 m/s) turbidity currents are driven by a dense (10-30% concentration) near-bed layer at their front, which needs inclusion in flow modelling, whilst slower flows are entirely dilute.
- This dense frontal layer sometimes erodes large sediment volumes (as for ignition), yet maintains a near-uniform speed (as for autosuspension), leading to a new (travelling wave) model for flow behaviour.
- Monitoring shows how flows sculpt canyons and channels via supercritical bedforms (cyclic steps) and extremely fast-moving knickpoints that are internally generated, and how deposits record flow processes (e.g. cyclic steps).

Glossary

Turbidity current: An underwater avalanche of sediment and water that is denser than the surrounding water, and thus moves down-slope along the ocean or lake floor.

Turbidite: Layer of sand and mud that has settled out from a turbidity current to form a deposit on the ocean or lake floor.

Ignition: Positive feedback leading to acceleration of a turbidity current due to seafloor erosion that causes the flow to become even faster and denser, leading to more erosion.

Autosuspension: A near-equilibrium state that occurs when settling of sand and mud from a turbidity current is balanced by seafloor erosion, leading to near uniform flow velocity.

Dissipation: Negative feedback loop leading to deceleration of a turbidity current, as settling of sand and mud causes the flow to become less-dense and slower, causing further settling.

Acoustic Doppler current profiler (ADCP): Sensor emitting a sound-pulse that is scattered from sand and mud particles within a turbidity current, which measures the speed of those particles at different heights above the seabed to produce a velocity profile.

Frontal cell: The frontal part of faster-moving (> ~1.5 m/s) turbidity current that is faster than the rest of the flow, and contains a near-bed layer with high sediment concentrations.

Knickpoint: An abrupt step in a submarine channel or canyon profile that resembles a water-fall.

Supercritical flow: Flows can exist in two basic states that are either thin-and-fast (‘supercritical’) flow or thick-and-slow (‘subcritical’) flow, which are separated by a hydraulic jump.

Submarine fan: A large-scale accumulation of sediment formed by turbidity currents that comprises a canyon, channel with levees, and lobe at the end of the channel.

Submarine canyon: A valley that is deeply incised into the seafloor through which turbidity currents flow, which is much deeper than a submarine channel.

Submarine channel: A channel that is less deeply incised into the seafloor through which turbidity currents flow, whose upraised flanks (called levees) may lie above the surrounding seabed.

Levee: Upraised flanks of a submarine channel that lie above the surrounding seafloor, which are formed by overspill of turbidity currents from the channel.

Lobe: Area that lies beyond the end of a submarine channel, where turbidity currents expand, and which is often characterised by unusually rapid sediment deposition and scours.

Figures

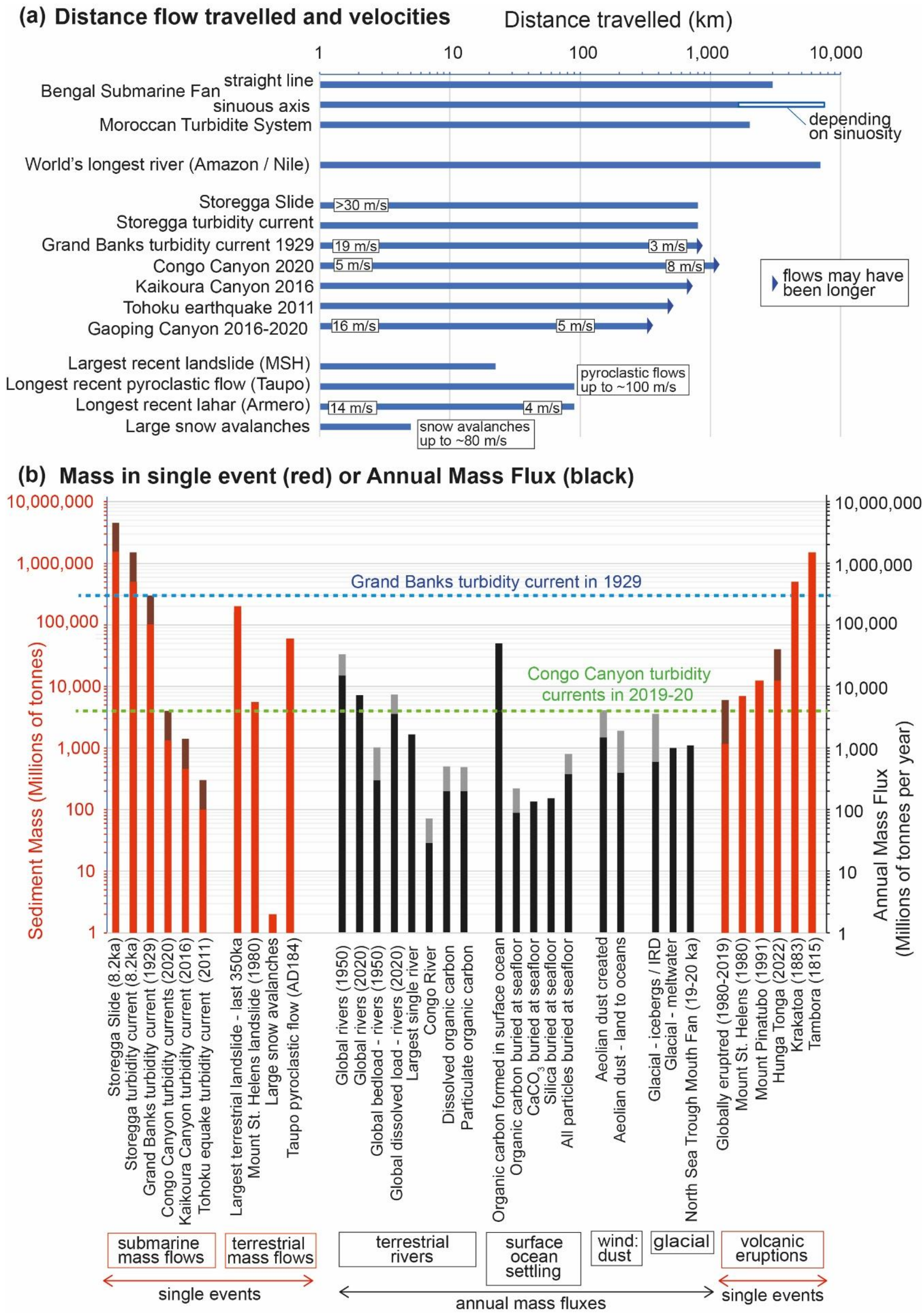

(a) Distance flow travelled and velocities
Distance travelled (km)
1
10
100
1,000
10,000
Bengal Submarine Fan
straight line
sinuous axis
Moroccan Turbidite System
depending on sinuosity
World's longest river (Amazon / Nile)
Storegga Slide
>30 m/s
Storegga turbidity current
Grand Banks turbidity current 1929
19 m/s
3 m/s
Congo Canyon 2020
5 m/s
8 m/s
Kaikoura Canyon 2016
Tohoku earthquake 2011
Gaoping Canyon 2016-2020
16 m/s
5 m/s
flows may have been longer
Largest recent landslide (MSH)
Longest recent pyroclastic flow (Taupo)
pyroclastic flows up to ~100 m/s
Longest recent lahar (Armero)
14 m/s
4 m/s
Large snow avalanches
snow avalanches up to ~80 m/s
(b) Mass in single event (red) or Annual Mass Flux (black)
Sediment Mass (Millions of tonnes)
Annual Mass Flux (Millions of tonnes per year)
10,000,000
1,000,000
100,000
10,000
1,000
100
10
1
Grand Banks turbidity current in 1929
Congo Canyon turbidity currents in 2019-20
Storegga Slide (8.2ka)
Storegga turbidity current (8.2ka)
Grand Banks turbidity current (1929)
Congo Canyon turbidity currents (2020)
Kaikoura Canyon turbidity current (2016)
Tohoku equake turbidity current (2011)
Largest terrestrial landslide - last 350ka
Mount St. Helens landslide (1980)
Large snow avalanches
Taupo pyroclastic flow (AD184)
Global rivers (1950)
Global rivers (2020)
Global bedload - rivers (1950)
Global dissolved load - rivers (2020)
Largest single river
Congo River
Dissolved organic carbon
Particulate organic carbon
Organic carbon formed in surface ocean
Organic carbon buried at seafloor
$CaCO_3$ buried at seafloor
Silica buried at seafloor
All particles buried at seafloor
Aeolian dust created
Aeolian dust - land to oceans
Glacial - icebergs / IRD
Glacial - meltwater
North Sea Trough Mouth Fan (19-20 ka)
Globally eruptred (1980-2019)
Mount St. Helens (1980)
Mount Pinatubo (1991)
Hunga Tonga (2022)
Krakatoa (1883)
Tambora (1815)
submarine mass flows
terrestrial mass flows
terrestrial rivers
surface ocean settling
wind: dust
glacial
volcanic eruptions
single events
annual mass fluxes
single events

Figure 1. Comparison between turbidity currents and various other major global sediment transfer processes, showing turbidity current are one of the most important sediment transfer processes ('pumps') on Earth. (a) Distance that flows travel (km) and their velocities (m/s). **(b)** Mass of sediment carried by individual events (in red), and as annual sediment mass fluxes (in black), with uncertainties as grey additional bars. The sediment mass carried by the Grand Banks turbidity current in 1929 (blue dotted line; [3]) and Congo Canyon turbidity currents in 2020 (green dotted line; [4]) are indicated. Supplementary Table 1 provide further information and lists source literature used for the distances, speeds, masses or annual mass fluxes that are quoted.

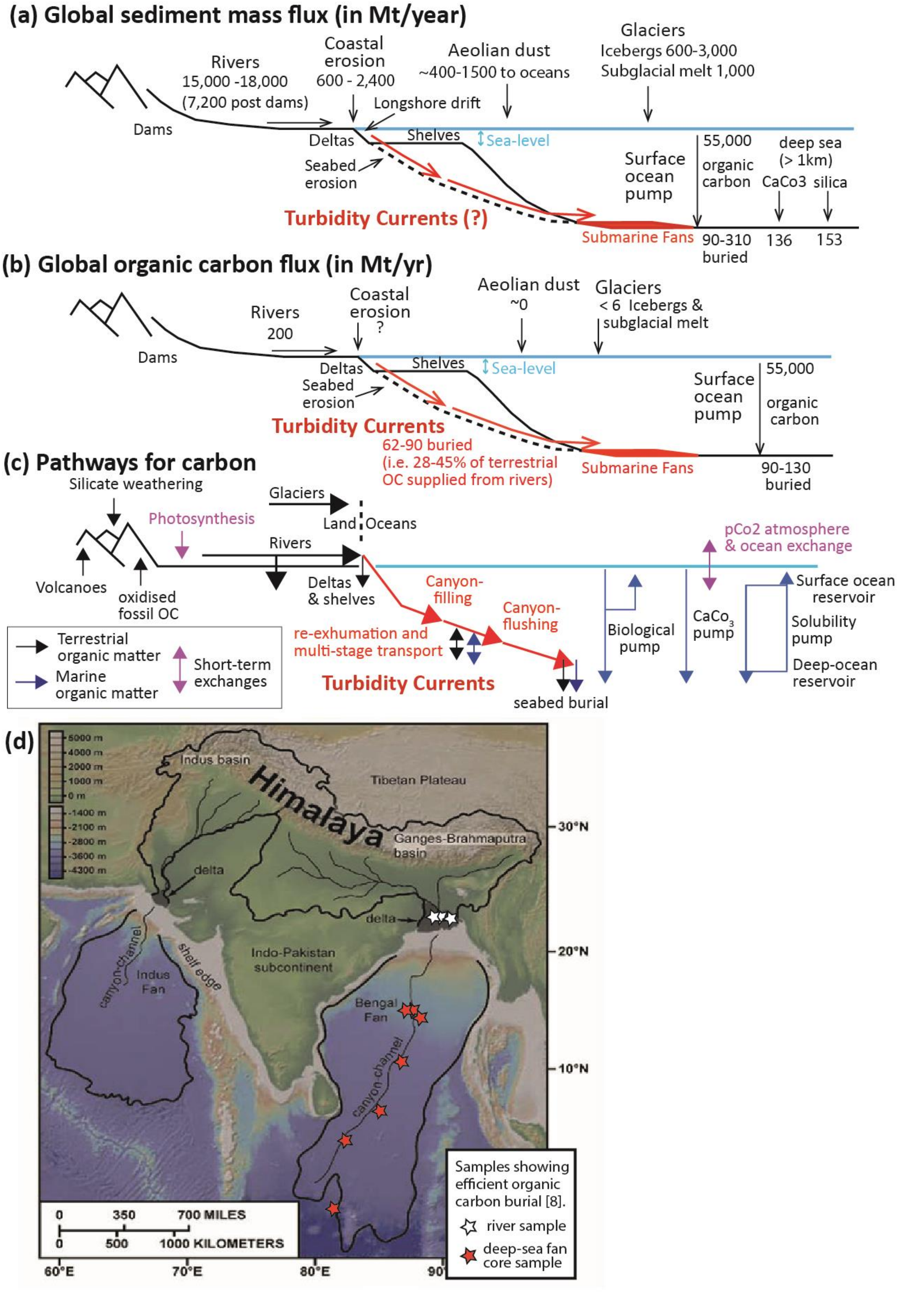

Figure 2. Turbidity current play a globally important role in organic carbon burial. (a) Global sediment mass fluxes (in Mt/yr; see Figure 1 and Supplementary Table 1 for original

data sources). **(b)** Global organic carbon mass fluxes (in Mt/yr). A future grand challenge is to quantify global sediment and organic carbon fluxes in turbidity currents [14]. **(c)** Pathways for global organic carbon cycling. Burial of organic carbon by turbidity currents affects atmosphere pCO_2 and thus climate, but over long term (> 1 ka) time scales. Terrestrial organic carbon pathways in black, and marine organic carbon pathways in blue. Processes that exchange carbon with atmosphere on short term in purple. Estimate of terrestrial organic carbon burial (62-90 MtC/yr) in marine sediments by turbidity currents is from [14]. **(d)** Burial of organic carbon by turbidity currents can be highly efficient, such as within the huge Bengal Submarine Fan [8]. Organic carbon types and amounts in river samples (white stars) resemble those in deep-sea cores (red stars). Bathymetry data reproduced from the GEBCO_2021 Grid, www.gebco.net

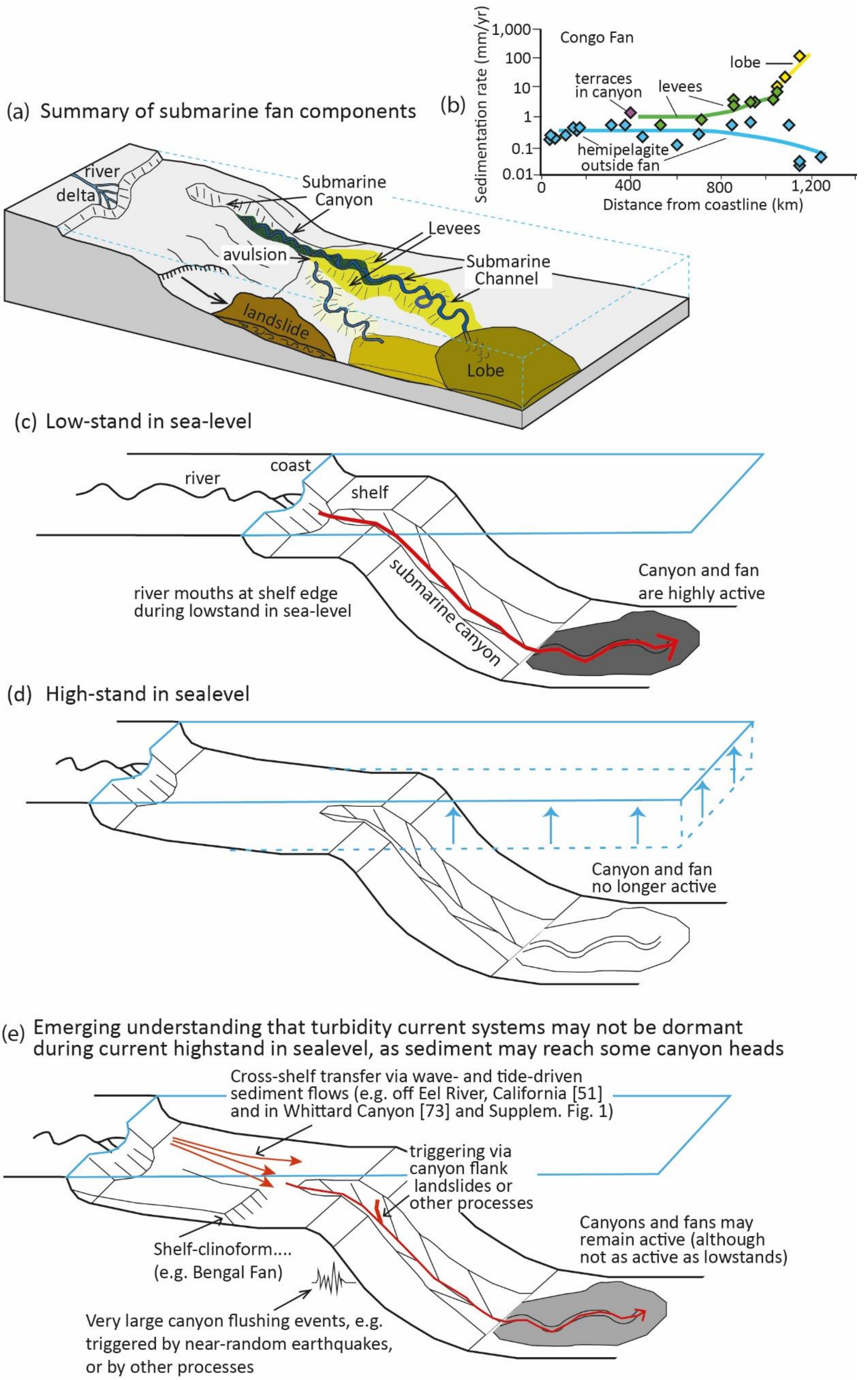
(a) Summary of submarine fan components
river
delta
Submarine
Canyon
Levees
avulsion
Submarine
Channel
landslide
Lobe
(b)
Congo Fan
Sedimentation rate (mm/yr)
1,000
100
10
1
0.1
0.01
lobe
terraces
in canyon
levees
hemipelagite
outside fan
0
400
800
1,200
Distance from coastline (km)
(c) Low-stand in sea-level
river
coast
shelf
submarine canyon
river mouths at shelf edge
during lowstand in sea-level
Canyon and fan
are highly active
(d) High-stand in sealevel
Canyon and fan
no longer active
(e) Emerging understanding that turbidity current systems may not be dormant
during current highstand in sealevel, as sediment may reach some canyon heads
Cross-shelf transfer via wave- and tide-driven
sediment flows (e.g. off Eel River, California [51]
and in Whittard Canyon [73] and Supplem. Fig. 1)
triggering via
canyon flank
landslides or
other processes
Shelf-clinoform....
(e.g. Bengal Fan)
Canyons and fans may
remain active (although
not as active as lowstands)
Very large canyon flushing events, e.g.
triggered by near-random earthquakes,
or by other processes

Figure 3. Submarine fans and frequency of turbidity current activity. (a) Summary of the main elements of a submarine fan. **(b)** Sedimentation rates in different parts of the Congo Submarine Fan (after [124]). **(c)** At glacial low-stands in sea-level, most river mouths will connect directly to submarine canyon-heads [67,68], so that turbidity currents are highly active on submarine fans [66,70]. This is also the case for the small number of modern canyon-heads that connect directly to river mouths (e.g. Congo Canyon [4] or Gaoping Canyon [9,41,42]). **(d)** Previous sequence (e.g. stratigraphic models) proposed that submarine canyons are dormant during high-stands in sea-level [66], as river mouths are separated from most canyon heads. **(e)** However, there is an emerging view that turbidity current systems are surprisingly active during the present day high-stand in sea-level [70]. For example, turbidity currents occur in Whittard Canyon, despite being 300 km from the nearest coast [69], and flows occur for 30% of the time in the upper Congo Canyon [36, 37] (Supplementary Fig. 2). Sediment can also be transferred efficiently across the shelf via wave or tide action to the canyon head (e.g. Eel Shelf in California) [73,74], or via progradation of large clinoforms (e.g. Bengal Fan in the Bay of Bengal) [72].

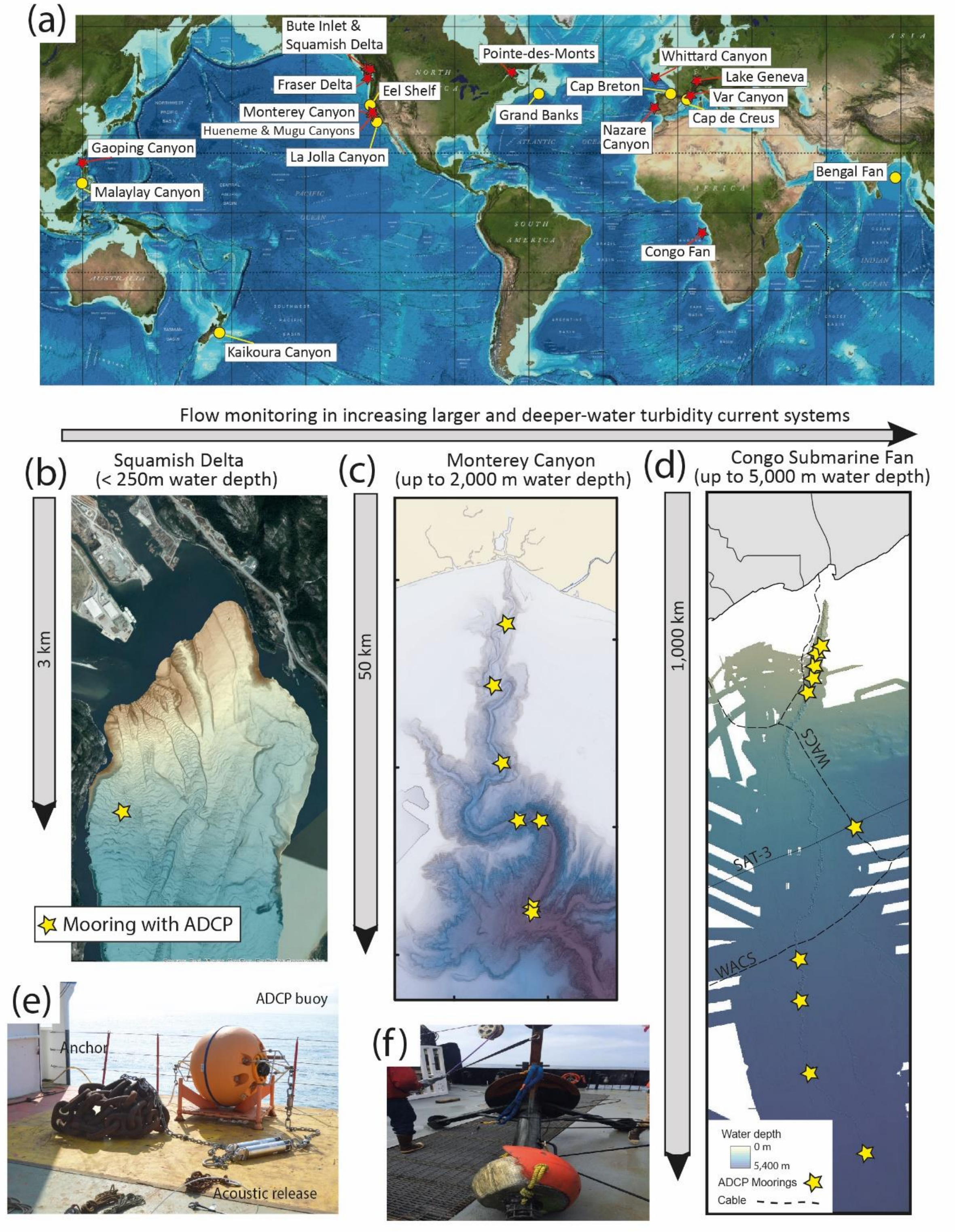

Figure 4. Direct monitoring of turbidity currents. (a) Map of just ~12 locations (red stars) worldwide where turbidity currents have currently been monitored in detail [27-54,61,69, 125-126] and other key locations (yellow circles) mentioned in the text. Image reproduced from the GEBCO world map 2014, www.gebco.net. Flow monitoring has moved from **(b)** smaller systems in shallow water such as Squamish Delta [38-39,50,59,61,115] where

logistic are easier, to **(c)** larger systems in moderate depths such as Monterey Canyon [34,35,51-52,60,87], and **(d)** finally very large systems in deep-water such as the Congo Fan, where turbidity currents broke the WACs and SAT-3 telecommunication cables (dotted lines) in 2020 and 2021 [4,36,37]. **(e)** These studies included moorings with an acoustic Doppler current meter (ADCP) in a buoyant float connected to a heavy (e.g. 1 tonne) anchor via a wire or chain, and recovered by remote triggering of an acoustic release [118]. Mooring shown here is on deck of a research vessel before deployment in Congo Canyon. **(f)** Heavy frame weighing 800 kg that slid for ~7 km down Monterey Canyon at speeds of up to 4.4 m/s [35,52]. It moved at a similar speed to much smaller objects, suggesting that they were rafted in a dense near-bed layer [35,52].

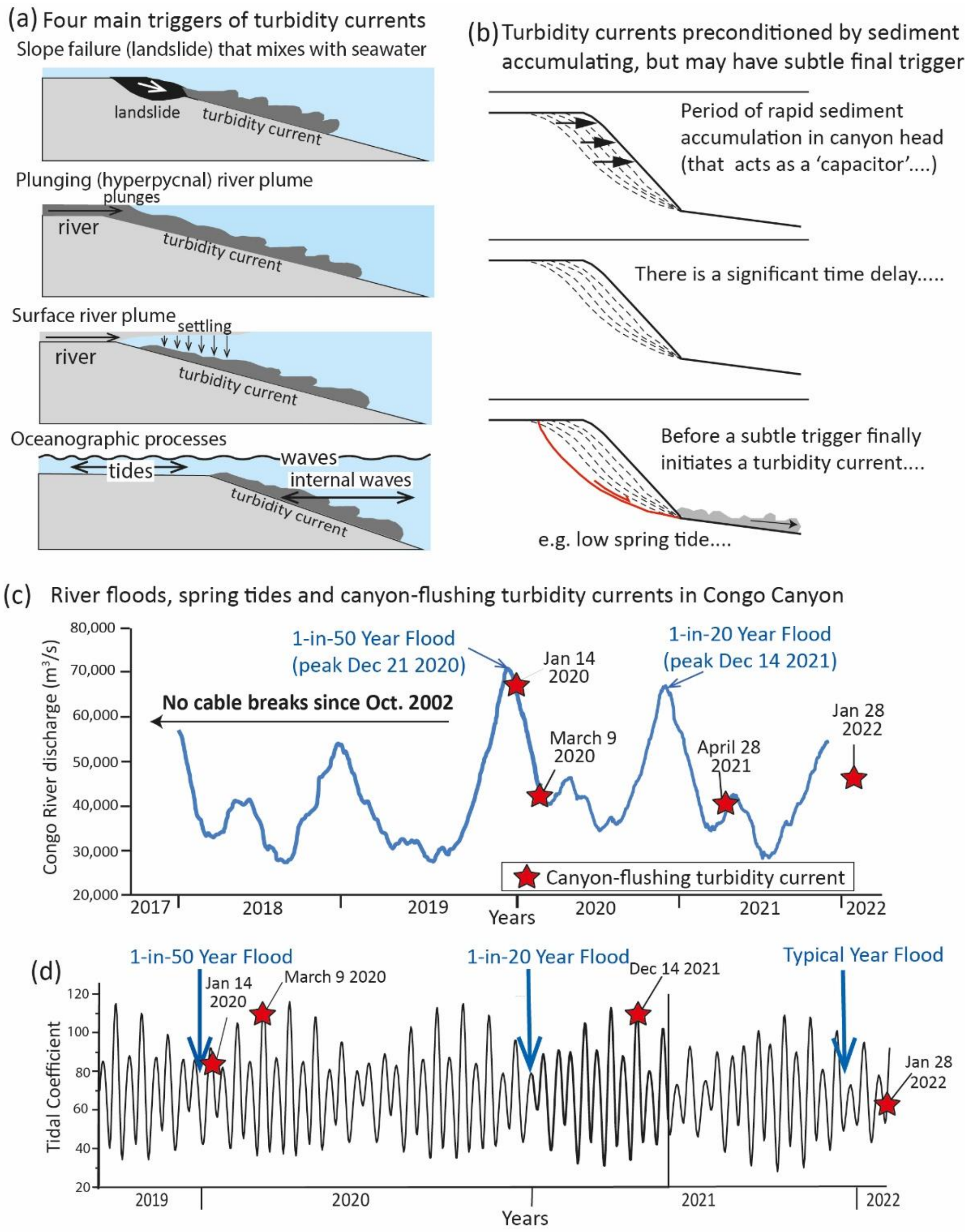

Figure 5. New insights into causes of turbidity currents. (a) Four main causes of turbidity currents [55,56] are (i) slope failures (landslides), (ii) plunging of hyperpycnal river plumes that have high enough sediment concentrations to be denser than seawater [57], and (iii) sediment settling from surface river plumes [39,47-48,58]. It has emerged that surface river plumes with very low (< 0.07 g/l) sediment concentrations can generate turbidity currents [39], such that turbidity currents may occur offshore a wider range of rivers than once thought. (iv) Oceanographic processes such as storm waves, tides and internal waves that can

supply sediment to canyon heads and trigger flows (including via landslides). **(b)** Significant time delays may occur between periods of rapid sediment accumulation in canyon heads, and final triggering of turbidity currents by subtle external triggers [4,60-61]. **(c,d)** River floods and tides combine to generate turbidity currents at many sites worldwide, including four extremely powerful turbidity currents (red stars) that flushed the Congo Canyon in 2020-2022 [4,5]. This cluster of canyon-flushing turbidity currents are associated with major floods along the Congo River, but occurred several weeks to months after the flood peaks, often at spring tides [4,5].

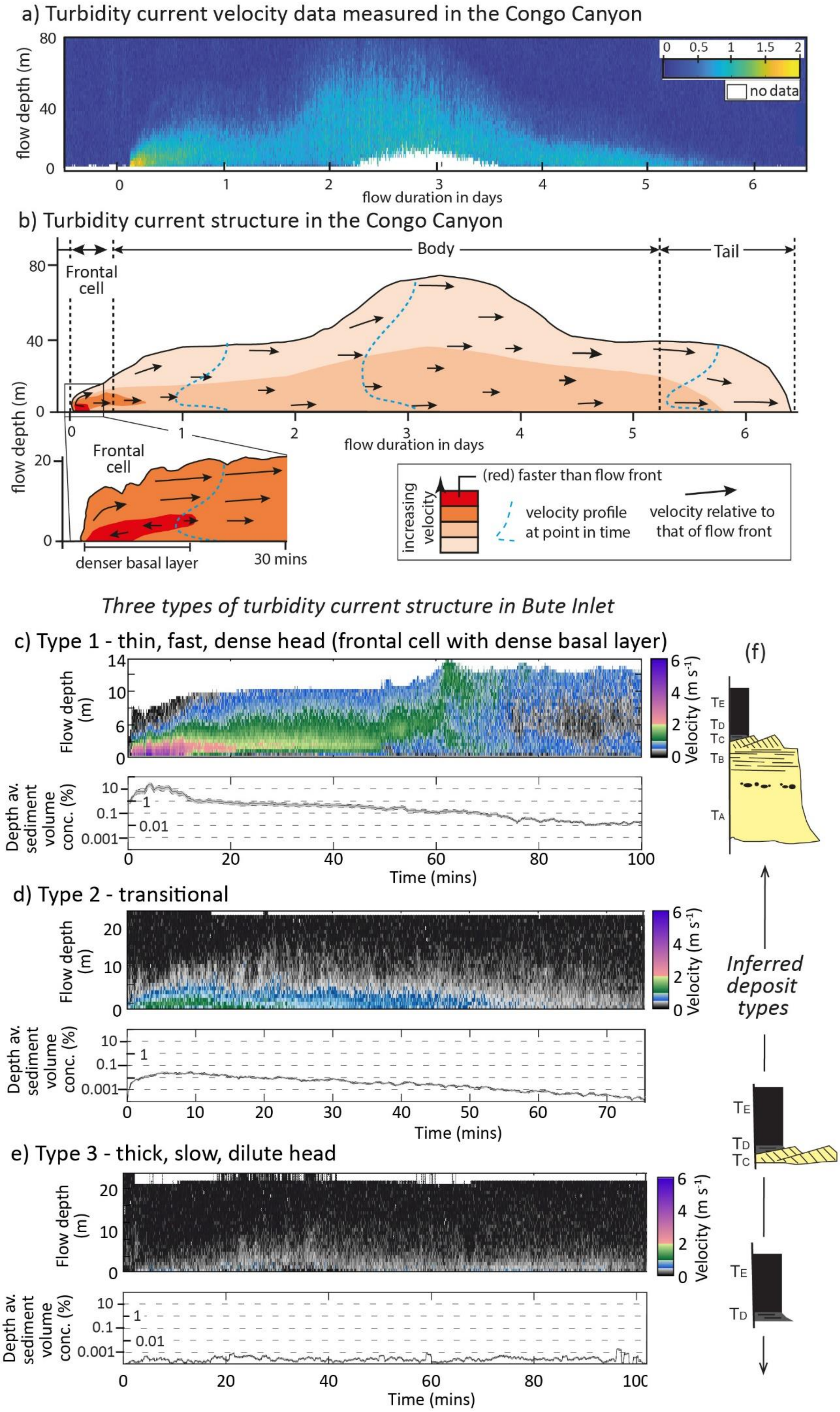

a) Turbidity current velocity data measured in the Congo Canyon
flow depth (m)
flow duration in days
no data
b) Turbidity current structure in the Congo Canyon
Frontal cell
Body
Tail
flow depth (m)
flow duration in days
denser basal layer
30 mins
(red) faster than flow front
increasing velocity
velocity profile at point in time
velocity relative to that of flow front
Three types of turbidity current structure in Bute Inlet
c) Type 1 - thin, fast, dense head (frontal cell with dense basal layer)
Flow depth (m)
Velocity (m s-1)
Depth av. sediment volume conc. (%)
Time (mins)
d) Type 2 - transitional
e) Type 3 - thick, slow, dilute head
(f)
TE
TD
TC
TB
TA
Inferred deposit types

Figure 6. New insights into internal structure of turbidity currents. (a) Velocity time-series of a turbidity current in Congo Canyon measured by an ADCP mooring [after 36]. **(b)** Summary of velocity structure of Congo Canyon turbidity currents. They comprise a near-bed frontal zone (‘frontal cell’) that is faster and denser than the rest of the flow, and runs away from a trailing body and tail, causing the flow to stretch [36]. This structure differs from laboratory flows in which a faster body feeds a slower head [33]. **(d-f)** Three types of turbidity currents observed in Bute Inlet. Plots show time-series of velocity and layer-average sediment volume concentration derived via the Chezy equation [after 40]. Faster (>1.7 m/s) Type 1 flows have a frontal cell with a fast and dense near-bed layer, as in Congo Canyon flows. This dense layer drives the event and dominates sediment flux [40]. Slower Type 3 flows are entirely dilute, and lack a dense and fast frontal layer, whilst type 2 flows have intermediate speeds and sediment concentrations. A single turbidity current may evolve from Type 1 to Types 2 and 3 as it decelerates [40]. (f) Inferred types of turbidite deposit likely formed by different types of flow, with Bouma sequence intervals (T_A to T_E) marked [40].

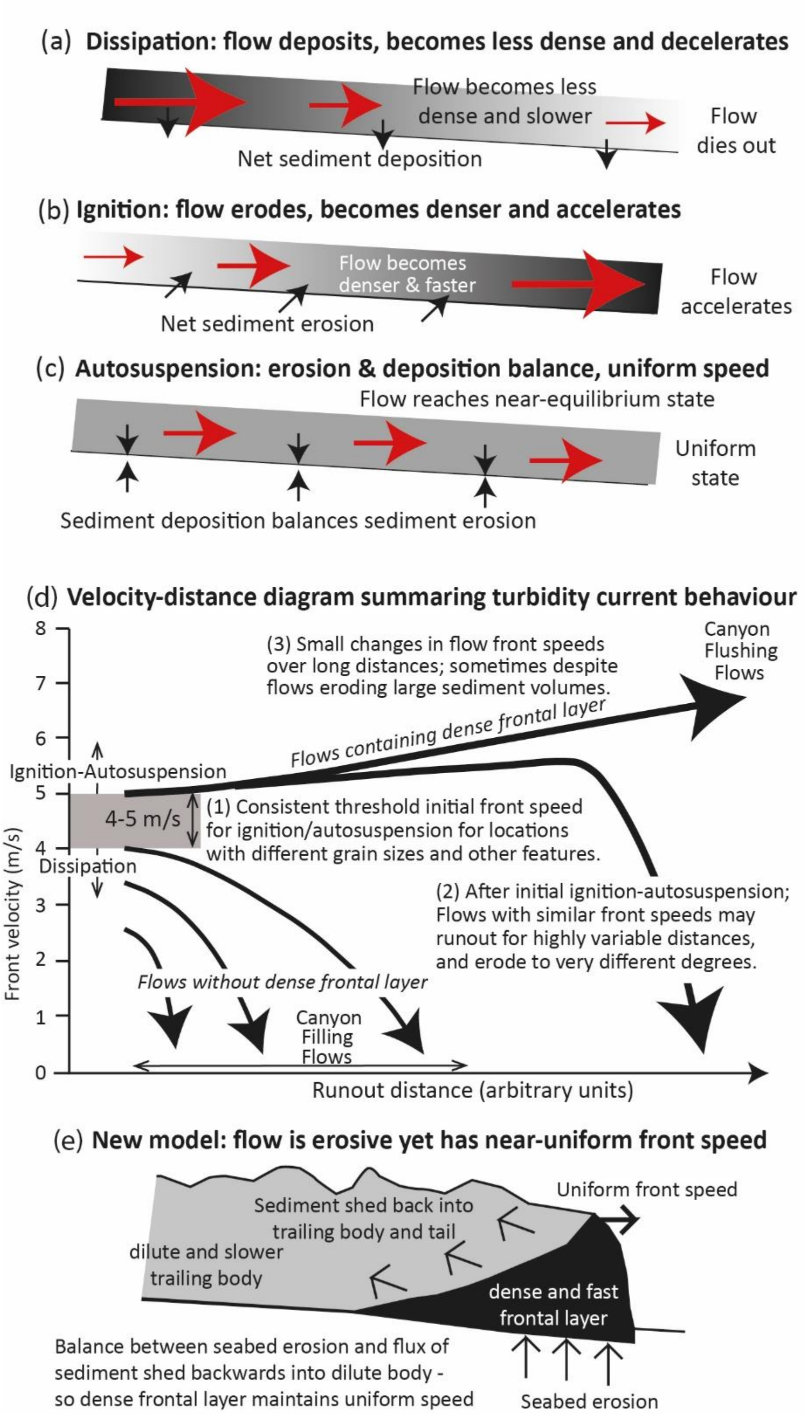

Figure 7. A new view of how turbidity currents behave. Past models inferred flows either **(a)** deposited sediment and dissipated; **(b)** eroded, became denser and faster, and accelerated (ignited); or **(c)** balanced erosion and deposition to create a near-equilibrium uniform velocity (autosuspending) state [25]. Red arrows denote flow speed; black arrows are sediment exchange with the bed. **(d)** Summary of changes in flow front speeds seen in direct field measurements, showing how flow behaviour diverges if an initial threshold speed of 4-5 m/s

is exceeded [4,87]. The threshold speed is independent of dominant sediment grain size. **(e)** New 'travelling wave' model in which flows may both erode the seabed (as in ignition) and sustain near uniform speeds for long distances (as in autosuspension) [4,87]. The flow contains a dense frontal layer in which seabed erosion is balanced by sediment shed back into a dilute trailing body.